

**FABRICATION AND CHARACTERISATION OF  
DYE-SENSITISED SOLAR CELL**

**CHAI SEOK YIAN**

**A project report submitted in partial fulfilment of the  
requirements for the award of the degree of  
Bachelor (Hons.) of Material and Manufacturing Engineering**

**Faculty of Engineering and Science  
Universiti Tunku Abdul Rahman**

**May 2011**

## DECLARATION

I hereby declare that this project report is based on my original work except for citations and quotations which have been duly acknowledged. I also declare that it has not been previously and concurrently submitted for any other degree or award at UTAR or other institutions.

Signature : \_\_\_\_\_

Name : \_\_\_\_\_Chai Seok Yian\_\_\_\_\_

ID No. : \_\_\_\_\_07UEB04448\_\_\_\_\_

Date : \_\_\_\_\_

**APPROVAL FOR SUBMISSION**

I certify that this project report entitled “**FABRICATION AND CHARACTERISATION OF DYE-SENSITISED SOLAR CELL**” was prepared by **CHAI SEOK YIAN** has met the required standard for submission in partial fulfilment of the requirements for the award of Bachelor of Engineering (Hons.) Materials and Manufacturing Engineering at Universiti Tunku Abdul Rahman

Approved by,

Signature : \_\_\_\_\_

Supervisor: Assistant Professor Khaw Chwin Chieh

Date : \_\_\_\_\_

The copyright of this report belongs to the author under the terms of the copyright Act 1987 as qualified by Intellectual Property Policy of Universiti Tunku Abdul Rahman. Due acknowledgement shall always be made of the use of any material contained in, or derived from, this report.

© 2011, Chai Seok Yian. All right reserved.

Specially dedicated to  
My beloved, father and mother

## ACKNOWLEDGEMENTS

I would like to thank the faculty, Faculty Engineering and Science for giving me the opportunity and platform for challenging myself with this project.

I would like to thank everyone who had contributed to the successful completion of this project. First of all, I would like to express my sincere gratitude and deep thanks to my research supervisor, Dr. Khaw Chwin Chieh and co-supervisor Dr. Liang Meng Suan for their valuable advice, guidance, support and his enormous patience throughout the development of the research.

Besides, I would like to take this opportunity to show my deepest appreciation and gratitude to my teammate, Oon Yen Han for her advice, valuable suggestion and comments given by her time to time. Besides, I would like to convey my sincere thanks to all lab assistances from the chemical lab and mechanical lab for his/her valuable assistances of the research.

In addition, I would also like to express my gratitude to my loving parent and friends who had helped, support and given me encouragement to complete my project thesis.

## FABRICATION AND CHARACTERISATION OF DYE-SENSITISED SOLAR CELL

### ABSTRACT

Dye-sensitised solar cell (DSSC) is a promising efficient low-cost molecular photovoltaic device. One of the key components is the dye/sensitizer, responsible for capture of sunlight. Many researches have been conducted to produce high efficient cell. Hence the purpose of this project is to investigate the effect of dyes on the efficiency of DSSC in the search for better performance solar cell. In this project, two Ruthenium metal complex dyes are characterised using Current-Voltage (I-V) test, Ultraviolet (UV) Visible spectroscopy, X-ray diffraction (XRD), Scanning Electron Microscopy (SEM) and Energy-dispersive Spectroscopy (EDS). It is found that the DSSC with N719 sensitiser gives better photovoltaic performance than that of the N3 sensitiser. I-V studies show that the most significant factor that affected the DSSC efficiency is the  $J_{sc}$  ; 16.89 mA/cm<sup>2</sup> for N719 sensitiser while only 14.51 mA/cm<sup>2</sup> for the N3 sensitiser. Hence, the N719 (8.43%) DSSC has to higher efficiency than that of N3 sensitiser (6.58%). Besides, N719-DSSC able to adsorb more dye molecules as compared to the N3-DSSC as indicated by the UV test result. The more dye molecules adsorbed the higher efficiency DSSC will be. TiO<sub>2</sub>-anatase phase is detected by the x-ray studies in the project and anatase-phase gives high efficiency than other phases. In addition, the dye soaking time is also investigated in this project. From the I-V test shows that the optimal efficiency obtained for both two dyes (N719 = 8.53%, N3 = 6.61%) is at 24 hour immersion times. This is supported by the the maximal bands of the Metal ligand charge transfer (MLCT) of both Ru dyes are obtained with 24 hours immersion periods. This means that the full dye coverage is able to obtain at 24 hours immersion periods.

## TABLE OF CONTENTS

<b>DECLARATION</b>	<b>ii</b>
<b>APPROVAL FOR SUBMISSION</b>	<b>iii</b>
<b>ACKNOWLEDGEMENTS</b>	<b>vi</b>
<b>ABSTRACT</b>	<b>vii</b>
<b>TABLE OF CONTENTS</b>	<b>viii</b>
<b>LIST OF TABLES</b>	<b>xi</b>
<b>LIST OF FIGURES</b>	<b>xii</b>
<b>LIST OF SYMBOLS / ABBREVIATIONS</b>	<b>xiv</b>
<b>LIST OF APPENDICES</b>	<b>xv</b>

### CHAPTER

<b>1</b>	<b>INTRODUCTION</b>	<b>1</b>
	1.1 Green Technology	1
	1.2 History of Solar cell	2
	1.3 Dye-Sensitised Solar Cell (DSSC)	3
	1.3.1 Structure of DSSC	3
	1.3.2 Basic Operating Principles of DSSC	3
	1.3.3 Advantages of DSSC	4
	1.3.4 Application of DSSC	5
	1.4 Aim and Objectives	5
	1.5 Flow of Report	5
<b>2</b>	<b>LITERATURE REVIEW</b>	<b>6</b>



2.1	Introduction	6
2.2	Dye / Sensitizer	7
2.2.1	Ruthenium Polypyridyl Complexes (Ru Complexes)	7
2.3	Nanocrystalline Oxide Semiconductors	14
2.3.1	Titanium Oxide (TiO <sub>2</sub> )	14
<b>3</b>	<b>METHODOLOGY</b>	<b>22</b>
3.1	Introduction	22
3.2	Raw Materials and Apparatus	22
3.3	DSSC Preparation and Fabrication	25
3.4	Equipment	27
3.4.1	Current-Voltage (I-V) Tester	27
3.4.2	UV (Ultra-Violet) Visible Spectrophotometer	28
3.4.3	X-ray diffraction (XRD)	29
3.4.4	Scanning Electron Microscope (SEM) and Energy Dispersive Spectroscopy (EDS)	30
<b>4</b>	<b>RESULTS AND DISCUSSION</b>	<b>31</b>
4.1	Characterisation of DSSC with different Dye/Sensitiser	31
4.1.1	I-V Test	31
4.1.2	Morphology and Composition Studies	38
4.1.3	X-Ray Diffraction Study	41
4.1.4	Dye Loading	44
4.2	Characterisation of DSSC with different Dye Adsorption Time	48
4.2.1	I-V Test	48
4.2.2	Dye Loading	53
<b>5</b>	<b>CONCLUSION AND RECOMMENDATIONS</b>	<b>57</b>
5.1	Conclusion	57
5.1.1	Characterisation of DSSC for different Sensitisers	57
5.1.2	Effect of Dye Loading	58

		x
5.2	Problems Encountered and Solutions	59
5.3	Recommendations	61
<b>REFERENCES</b>		<b>62</b>
<b>APPENDICES</b>		<b>67</b>

**LIST OF TABLES**

<b>TABLE</b>	<b>TITLE</b>	<b>PAGE</b>
2.1	Comparison of Ru (II) based complexes dyes	10
3.1	Introduction of raw materials for DSSC	23
3.2	Apparatus	24
4.1	Photovoltaic characteristic for different sensitiser, N3 and N719	32
4.2	Photovoltaic characteristic of N3 for first and second day measurement	35
4.3	Photovoltaic characteristic of N719 for first and second day measurement	36
4.4	Photovoltaic performance of different DSSC with N3	37
4.5	HOMO-LUMO energies of N3 and N719 dyes	45
4.6	Photovoltaic performance of DSSC with N3 sensitiser at different dye adsorption time	48
4.7	Photovoltaic performance of DSSC with N719 sensitiser at different dye adsorption time	51
4.8	Adsorption bands and absorbance of TiO <sub>2</sub> /N3 at different immersion time	54
4.9	Adsorption bands and absorbance of N719/TiO <sub>2</sub> at different immersion time	56

**LIST OF FIGURES**

<b>FIGURE</b>	<b>TITLE</b>	<b>PAGE</b>
3.1	Process flow chart for fabrication of DSSC	26
3.1	IV-tester	27
3.2	UV (Ultra-Violet) Visible Spectrophotometer	28
3.3	X-ray diffraction (XRD)	29
3.4	Scanning Electron Microscope (SEM) and Energy Dispersive Spectroscopy (EDS)	30
4.1	Current-to-voltage curve with N3 and N719 sensitisers.	31
4.2	I-V curve with N3 for first and second day measurement	35
4.3	I-V curve with N719 for first and second day measurement	36
4.4	I-V characteristic of different DSSC with N3	37
4.5	SEM micrographs of TiO <sub>2</sub> film (a) 1300X magnification (b)110X magnification	38
4.6	SEM micrograph and EDS data for 20 nm TiO <sub>2</sub> film	39
4.7	SEM micrograph and EDS data for 20 nm N3/TiO <sub>2</sub> film	39
4.8	SEM micrograph and EDS data for 20 nm N719/TiO <sub>2</sub> film	39

4.9	X-ray diffractogram of TiO <sub>2</sub> film	41
4.10	X-ray diffractogram of TiO <sub>2</sub> (Blue line), N3/TiO <sub>2</sub> (blue line) and N719/ TiO <sub>2</sub> (black line)	42
4.11	UV-visible spectroscopy for N3 and N719 dye solution	44
4.12	Energy level diagram for DSSC by using N3 and N719	46
4.13	Variation of <i>V<sub>oc</sub></i> and <i>J<sub>sc</sub></i> with time for N3-DSSC	49
4.14	Variation of efficiency with time for N3-DSSC.	50
4.15	Variation of <i>V<sub>oc</sub></i> and <i>J<sub>sc</sub></i> with time for N719-DSSC	52
4.16	Variation of efficiency with time for N719-DSSC	52
4.17	Absorption spectra of TiO <sub>2</sub> /N3	53
4.18	Absorption spectra of N719/TiO <sub>2</sub> at different immersion time	55
5.1	Electrolyte leakages from poor cell assembly	59
5.2	Remove excess electrolytes by tissue.	60

**LIST OF SYMBOLS / ABBREVIATIONS**

DSSC	Dye-Sensitized Solar Cells
$J_{sc}$	Current density, m A/cm <sup>2</sup>
$V_{oc}$	Open voltage, mV
$FF$	Fill factor
$\eta$	Efficiency, %
$P_{in}$	Solar radiation intensity
$D$	Diffusion coefficient of electron
$\tau$	Electron lifetime
$L$	Electron diffusion length
$E_{cb}$	Conduction bands of the metal oxide, eV
$ns$	Nanoseconds, s
$\Delta E$	Energy gradient
EtOH	Ethanol
MeCN	Acetonitrile
CB	Conduction Band
VB	Valence Band
HOMO	Highest Occupied Molecular Orbital
LUMO	Lowest Unoccupied Molecular Orbital
NHE	Nitrogen Hydrogen Electrode
SCE	Saturated Calomel Electrode
LHE	Light harvesting efficiency
$F(\lambda)$	Incident light loss
$q$	Electron charge
$\Phi(\lambda)_{ET}$	Electron transfer yield
MLCT	Metal ligand charge transfer

**LIST OF APPENDICES**

<b>APPENDIX</b>	<b>TITLE</b>	<b>PAGE</b>
A	Molecules structure of N3 and N719 (Char, 2010)	67
B	Solvent Effect (Marinado, 2009)	68
C	X-ray pattern (Yang et al., 2009)	69
D	I-V Test result for N3 and N719 sensitizers	70
E	UV visible spectrophotometer result for N3 and N719 dye solution	71
F	EDS results for TiO <sub>2</sub> /N3 film and TiO <sub>2</sub> / N719 film	72
G	I-V Test results for DSSC with N3	73
H	I-V Test results for DSSC with N719	77

## CHAPTER 1

### INTRODUCTION

#### 1.1 Green Technology

At this century the world is in need of technology to provide sustainable energy to all population. Increasingly growth rate of the world population may implies enhanced diminishing of convention fossil source and their combustion products such as carbon dioxide and other greenhouse gases are likely contribute to the global warming, acid rain and pollution problems. Until recently, the problems caused by fossil fuels are conveniently ignored by policy makers, but it will lead difficulties for future generation. Therefore the renewable energy source such as biomass, solar, wind, waves, ocean and others are being considered as the possible energy sources to overcome the pollution and global warming problem.

Some of this alternative energy sources such as wind energy is limited by wind condition on long term basis and it may also cause noise pollution. Therefore, it is not being considered seriously in replacing fossil fuels as a dependable energy source. Besides, the ocean thermal energy conversion (OTEC) also impractical since it may alter and damage the ocean ecosystem because leakage of intermediate chemical into ocean. For the solar energy, there is radiant energy that produced by the sun itself. The sun makes energy in its inner core in a process called nuclear fusion. Solar energy is not only an environmentally friendly source of energy, it also as the most fundamental of sustainable energy sources that guarantee for billion of years. Solar cell is the device that able used to convert the solar energy into the electrical energy form.



## 1.2 History of Solar cell

Solar energy technologies can provide electrical generation by heat engine or photovoltaic means. The best known method for generating solar power are photovoltaic technology by using solar cell which can convert sunlight directly into electricity. This can simply be explained by quantum theory in which optical energy are converted into electric energy by interaction between photos and electrons in a solid.

In 1954, the first highly efficient solar cell was developed by Chapin, Fuller and Pearson by using a diffused silicon p-n junction. Nowadays, there are various types of the solar cells in the market. The three basic type solar cells are crystalline silicon, thin films concentrators and thermophotovoltaic solar cell. These cells are integrated to generate solar power plant components to make electricity. Normally, the photovoltaic panels are made either silicon or thin-film cells.

In the 1970s, research was conducted on photo-sensitisers for photographic used. The research involved the adsorption of dye on oxide semiconductors for the purpose of quantifying the dye-based spectral sensitization phenomena. This paved the way for the extraction of a photocurrent to an external circuit through the electrodes.

According to Kawakita (2009), the first dye-sensitised solar cell (DSSC) presented on the world, a cell from which an electric current can be taken out based on the electromotive force between the two electrodes, was developed in 1976. This cell was used porous zinc oxide as the dye supported. The energy conversion efficiency was 2.5%.

In 1991, Ecoles Polytechniques Federales de Lausanne (EPFL) presented prototype of current DSSC, which had an improved conversion efficiency of 7.12%. The characteristics of this prototype were titanium oxide nanoparticles which used to increase the dye absorption area to large scale and Ru-based dye with a wide range of optical absorption were developed. In 2009, the maximum cell conversion efficiency in measurement was 11.2%.

### 1.3 Dye-Sensitised Solar Cell (DSSC)

DSSC are currently the most efficient third-generation solar technology. DSSC which was proposed by O'Regan and Gratzel, has attracted considerable interest since 1991 because of its attractive properties, such as low production cost and low environmental impact during the fabrication. However, it has relatively low conversion efficiency (11.2%) as compare to the crystalline silicon (25.0%).

#### 1.3.1 Structure of DSSC

Typically, a DSSC consists of two electrodes dye-coated titanium oxide ( $\text{TiO}_2$ ) electrode as the anode and a Platinum (Pt) counter electrode as the cathode. These two electrodes were assembled into a sandwich type cell and sealed with hot-melt gasket. The porous layer of  $\text{TiO}_2$  nanoparticles with molecular dye able to absorb sunlight, similar to the function of chlorophyll in green leaves. The dye-coated titanium oxide was assembled with an electrolyte solution that containing iodide/triiodine redox couple. According to Lenzenmann and Kroon (2007), black dye, that consist of 4,9,14-tricarboxy 2,2'-6,6'-terpyridyl ruthenium (ii) trithiocyanate complex was the most efficient of dye, which strongly adsorbed visible light in the wavelength range of 400-900 nm.

#### 1.3.2 Basic Operating Principles of DSSC

When a photon from the sun was adsorbed by a dye molecule, an electron was excited bringing the dye to an electronically excited state ( $S^*$ ). Then, the excited electron was injected into conduction band of the metal oxide such as  $\text{TiO}_2$ . Actually, the electron was channelled into the ligand having the lowest  $\pi^*$  acceptor orbitals and electron injection into conduction band of the metal oxide taken place from there. Ideally, the photoinjected electron percolates through the nanoparticle networks which follow a random walk, and gets collected at the back-contact. While the

oxidised dye was regenerated to its ground state by taking an electron from the redox couple present in the electrolyte. The collected electrons travel through the external circuit, performing electrical work and eventually reach the counter electrode where they reduce the electron mediator species regenerating the reducing agents and complete the circuit. The energy level of the conduction band of nanoporous oxide semiconductor and redox level of iodine ions and triiodine should be situated between the excited level and ground level of the dye molecules.

### **1.3.3 Advantages of DSSC**

The DSSC offers a significant cost advantages over the conventional wafer-based silicon solar cell. This is because of the relatively inexpensive component materials and inherently simple device processing.  $\text{TiO}_2$  as a choice of the nanocrystalline oxide semiconductor because of it sensitised photochemistry stable and photo corrosion characteristics. Besides, it is cheaper, readily available in large quantity. Furthermore, it is relatively non-toxic, so it was suited with the environmental friendly and sustainable purpose. Silicon solar cell only able to capture the power when the light is intense while DSSC able to produce electricity in low light condition or even in the rainy day. This means that DSSC able to give better performance or higher efficient photovoltaic conversions compare to the conventional silicon cell photovoltaic technology. Besides, the colourable and transparent properties make it as factor widely selected for the decorative application where appearance is an important factor. The applications which require good appearance is hardly found in other type solar cell.

### **1.3.4 Application of DSSC**

Solar products are gradually become common now. Many products can be introduced by DSSC solar cell since the size easier modified and manufactured. Various modulud types of DSSC were developed, such as flexible light weight design on metal foil or plastic as well as the glass modulus. The products cover a broad range of low and high power application. Some important examples include solar garden lamps, street lights, pocket calculator, solar battery chargers, solar jackets, mobile electronics (phones and laptops), colourful decorative elements products, and others. Besides, it can also be directly incorporated into building by replacing conventional glass panel. These applications may indicate that human being reduced depletion and depending on the conventional fossil fuel.

## **1.4 Aim and Objectives**

Aim of this project is to fabricate the thin film dye-sensitised solar cell (DSSC) with high or comparable efficiency.

Objectives of this project are to:

- Investigate the effect of the sensitisers/dyes on the efficiency of DSSC.
- Investigate the effect of dye soaking time on the efficiency of DSSC.

## **1.5 Flow of Report**

A summary of the previous works or researches will be discussed in the literature review followed by the description of applied materials, equipment and methodology for DSSC fabrication. Then, the results of investigated factors will be reported and discussed. Lastly, the conclusions will be reported and recommendations for future work will be given.

## CHAPTER 2

### LITERATURE REVIEW

#### 2.1 Introduction

The natures of DSSC bring a unique feature, it separated the function of light adsorption from charge carrier transport. The dye molecules only absorbed the light and generated the charge carriers while the charge carried transport occurred in the oxide film and electrolyte. This implies the absence of minority carrier recombination, and hence a relatively high tolerance for impurity. However, the efficiency of DSSC still lower than the convention silicon solar cell. In order to maximise the energy conversion, all incoming photons are ideally converted to electrons without losing the energy of the photons.

Mori and Yanagida (2006) found that the incident photon to current conversion efficiency is determined by the light-harvesting efficiency (LHE), charge injection efficiency (CIE), charge collection efficiency (CCE). These factors are related with the parameters such as absorption coefficient of dye, thickness of dye-coated nanoporous semiconductors oxides, spatial distance between the surface of nanoporous semiconductors oxide and dye, electron diffusion length and others. Therefore, the characteristics of TiO<sub>2</sub> oxide films and dye/sensitiser will be discussed in this literature review.

## 2.2 Dye / Sensitizer

The efficiency of a DSSC largely depends on the charge generation step. Efficient dye has to fulfil certain requirements according to the study by Vougioukalakis, Philippopoulos, Stergiopoulos, and Falaras (2010). Firstly, dyes must have strong adsorption, preferably extending from the visible to the near-infrared. Secondly, the dyes must form a firm that irreversible adsorption (chemisorptions) to the semiconductor's surface and a strong electronic coupling between its excited state and the semiconductor conduction band. Lastly the dye must be chemically stable in the ground as well as in the excited and oxidized states, so that the DSSC will be stable over many years of exposure to sunlight.

### 2.2.1 Ruthenium Polypyridyl Complexes (Ru Complexes)

According to Hore, Vetter, Kern, Smit and Hinsch (2005), the transition metal coordination compounds, Ruthenium based metal organic complexes, are used as the effective dye due to their intense charge-transfer absorption in the whole visible range and high efficient metal to ligand charge transfer. The general formula of these ruthenium based metal organic complexes is  $\text{RuL}^1\text{L}^2\text{X}$ , where the  $\text{L}^1$  are 2,2',6'2-terpyridine compound having at least one group selected from a carboxyl group while the  $\text{L}^2$  represents a diketonate ligand and the X represent monodentate ligands selected from a halide, a cyano group or thiocyanate group.

Most well known Ru complexes were N3 (red dye), N794 (black dye), Z907 and N719. Many new dyes are chemically modified from N3 molecule on one of its two bipyridyl ligands. These new dyes may improve the molar absorption coefficient and long term stability of the DSSC such as K-series and Z907. Three dyes were discussed in this literature review, which are N3, N719 and black dye. Comparisons of  $J_{sc}$ ,  $V_{oc}$ ,  $FF$ , efficiency of these three different dyes are summarised in Table 2.1.

In 1993, the first Ru complexes dye used in Gratzel cell was tris(2,2'-bipyridyl-4,4'-carboxylate) ruthenium (Red dye) (N3 dye) developed by the Gratzel and his co-worker. The efficiency achieved of the cell was 7.1% under AM 1.5 irradiation. According to Thavasi, Renugopalakrishnan, Jose and Ramakrishna (2009), N3 has two bipyridine and two NCS ligands and the function of the carboxylate group in the dye is attached to the semiconductor oxide substrate by chemisorptions. In the study by Jang, Choi, Vittal, and Kim (2007), the efficiency of the DSSC with N3 was 5.7% only ( $J_{sc} = 14.60\%$ ,  $V_{oc} = 0.69$ ,  $FF = 0.57$ ). The highest efficiency of this dye was 7.12 % ( $J_{sc} = 12.0\%$ ,  $V_{oc} = 0.70$ ,  $FF = 0.68$ ) reported by Char in 2010. This improvement may due to the different dye absorption time; which in 24 hours immersion time periods. In the study of Uam, Jung, Jun and Kim (2010), the dye desorption varied as the function of the solvent and composition of the electrolyte. Thus, it is believed that the dye performance is affected by different type of electrolyte.

The N719 dye has been popularity used dye due to its outstanding performance. The highest record efficiency of 11.2% ( $J_{sc} = 17.7$ ,  $V_{oc} = 0.84$ ,  $FF = 0.74$ ) was reported by Gratzel (2003). This N719 dye has similar structure with the N3 dye but having tetrabutylammonium cation ( $(C_4H_9)_4N^+$  (TBA<sup>+</sup>) instead of H<sup>+</sup> at two carboxyl groups over four of them. This replacement increased the  $V_{oc}$  and  $J_{sc}$  of the DSSC as compared with N3 sensitiser. Thus, the overall efficiency of N719 was higher than the N3 sensitiser.

Besides, Hwong et al. (2007), Wu, Guo, Li, He and Hua (2010) and Kisserwan and Ghaddar (2010) also studied about the N719 sensitiser. The results obtained by these groups were 10.10%, 7.47%, and 6.50% respectively. All these groups result were significantly lower then the highest efficiency with an 11.2%. As the source of electrons, dyes should be strongly bonded to the surface of nanoporous semiconductor oxide for maximum electron injection and minimum recombination.

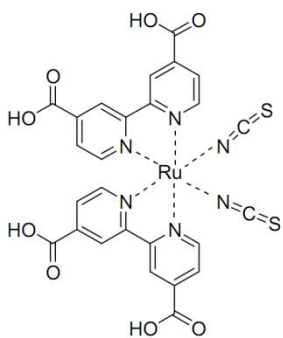
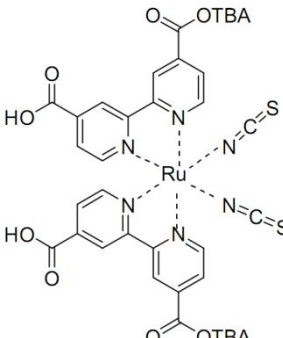
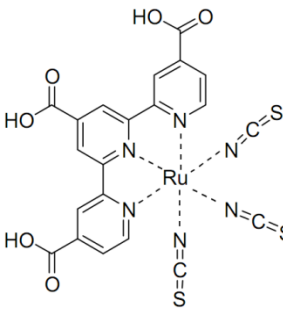
Composition electrolyte used by Gratzel (2003), Hwong, Wu et al. (2010), Kisserwan and Ghaddar (2010) were different. According to Shogo Mori and Shozo Yanagida (2006), different composition, concentration of the electrolyte and dye solution affected the overall performance of the DSSC. Hence, different  $J_{sc}$ ,  $V_{oc}$ ,  $FF$

and efficiency was obtained by different group although these groups were used the same dye. In the study of Mori and Yanagida (2006), electrolyte additive, tert-butylpyridine (TBP) able suppress the dark current, reduced dye aggregation on the TiO<sub>2</sub> surface, increase the photovoltage and long term stability. Hence, Hwong and his co-researchers obtained higher efficiency than other.

The structure of N749 is shown in Table 2.1. The overall efficiency of the DSSC with black dye were 10.40%, 7.10%, and 10.20% reported by Satyen (2005), Ogomi et al. (2010) and Yamaguchi, Uchida, Agatsuma, and Arakawa (2009), respectively. The best performance of this dye was reported by Chiba et al. (2006), with an overall efficiency of 11.1% ( $J_{sc}=20.9$ ,  $V_{oc}=0.74$ ,  $FF=0.72$ ). N749 sensitiser shows very high intensity photons conversion efficiency (IPCE) values in the visible range. This means that the N749 has potential greater performance the N3 and N719 dyes. However, Mori & Yanagida (2006) found that the absorption coefficient of N749 was lowers than N3 and N719 dye. Thus, the highest efficiency obtained by the N749 still slight lower than the N719.



Table 2.1: Comparison of Ru (II) based complexes dyes

Structure	Dye	$J_{sc}$ (mA/cm <sup>2</sup> )	$V_{oc}$ (V)	$FF$	Efficiency , $\eta$ (%)	Reference
	<b>N3</b> <b>(red dye)</b>	14.60	0.69	0.57	5.7	Jang et al. (2007)
		12.00	0.70	0.68	7.2	Hinsch et al. (2004)
	<b>N719</b>	17.70	0.85	0.75	11.20	Gratzel (2005)
		19.90	0.77	0.66	10.10	Hwang et al. (2007)
		16.10	0.69	0.67	7.47	Wu et al.(2010)
		16.20	0.60	0.67	6.50	Kisserwan and Ghaddar (2010)
	<b>N749</b> <b>(black dye)</b>	20.90	0.74	0.72	11.10	Chiba et al.(2006)
		21.00	0.69	0.70	10.20	Yamaguchi et al. (2007)
		18.96	0.63	0.60	7.10	Ogomi et al. (2010)
		20.53	0.72	0.71	10.40	Satyen (2005)

Despite many effort developed of high performance solar cells, their efficiency has not been improved dramatically. Thus, many studies of the primary processes in such cells have been conducted in order to determine the factors controlling their performance. One of the most important primary processes is electron injection. Interface characteristics are the critical factor for electron injection rate. Interface was the region formed when two phases (system) were in contact through which the intensive properties of one phase transfer to the other. Energetic interface was the region produce when two layering or interpenetrating of two or more materials of different valence and conduction bands or with dissimilar molecular energy level such as highest occupied molecular orbital (HOMO) and lowest unoccupied molecular orbital (LUMO).

There is two interface in DSSC sturcture, which are metal oxide/dye and metaloxide /dye/electrolyte. First is the metal oxide/dye. Upon light absorption, the dye reaches excited LUMO state and generated excitons, which diffuse into metal oxide/dye interface. MLCT occurs in which the electron was promoted from the molecules orbital (MO) of the metal center, ruthenium (filled  $t_{2g}$  level of 4d orbital) to a ligand-based MO (empty  $\pi^*$  orbital of the bipyridine ligands), resulting in the formation of oxidised  $Ru^{2+}$  and reduces ligands. Thus, dye/metal oxide interface designed such that the oxidation potential of excited dye (LUMO) is sufficiently negative to achieve efficient electron injection into the conduction band of metal oxide. Higher electron injection rate result higher  $J_{sc}$  and hence higher efficiency of the DSSC.

On the other hand, the oxidised dye must be generated by redox couple at the speed of nanoseconds ( $ns$ ) to kinetically compete with the metal oxide electrons for subsequent electron injection as well as to prevent the recombination, which depends on the energetic of metal oxide/dye/electrolyte interface. If the recombination rate is faster than the regeneration of dye, lower  $V_{oc}$  resulted. The coverage of sensitiser on nanocrystalline semiconductor film is also a factor of importance for controlling the electron loss (reaction between the injected electron and triiodine ions in an electrolyte). This is because such reaction occurs at the bare surface of the DSSC, which is confirmed by the observation that the lifetime of the injected electron decreases with decreasing dye coverage.

In order to reduce the effect, small additive molecules, 4-tert-butylpyridine (tBP), have been used as an adsorbate to cover the vacancies on the nanocrystalline semiconductor's surface. Another function of tBP is to increase the energy level of the conduction band edge,  $E_{CB}$ . In fact, tBP improves the  $V_{oc}$ ,  $FF$  of DSSC but the  $J_{sc}$  is often suppressed. In the study of Katoh, Fuke, Furub, Koide (2010), the electron injection efficiency decreased by 33% in a 1 M tBP solution. Besides, the absorbance decreased from 1.2 (0.5 hour) to 1 (2 hour). This indicated suppression of the electron injection efficiency.

Another important factor is an amount of sensitizer molecules which available for light harvesting and charge injection. Dye molecules are to be oriented on the surface of metal oxide with attachment functionalities of the molecule. Orientation reduces the covering area per absorbed molecules, providing a more compact and packed arrangement of the dye molecules, which allow for more adsorption dye of molecules. The rate constant for migration of excited energy would depend on the relative orientation of donor and acceptor moieties.

However, this is no longer possible if the dye adsorbed as aggregates. Problems of poor electron transfer to the metal oxide conduction band would be arisen if dyes are aggregated that results in an unsuitable energetic position of the LUMO level. Lower current density could be resulted by poor injection efficiency, due to unfavourable binding of dye onto the metal oxide surface. The orientation of the molecule on the metal oxide surface was characterised by anchoring group present in the dye.

Katoh et al. (2010) did a study by using the femtosecond TA spectroscopy, nonexponential ultrafast electron injection is observed in the 100 ps for N3 dyes adsorbed on  $TiO_2$  metal oxide films while 100 fs time range for  $TiO_2/N719$ . As compare these two dyes, the speed for electron injection for N719 is better than the N3. Thus, the  $TiO_2/N719$  interface also given higher efficiency as compared with  $TiO_2/N3$  interface.

In the study Katoh et al., the metal-to-ligand charge transfer (MLCT) absorption band shift slightly toward longer wavelengths with increasing concentration from 543 nm (0.5 hour) to 537 nm (2 hour). This peak position is affected by the intermolecular interaction between dye molecules. Reason for this shift slightly toward longer wavelength is because the adsorption of dyes is not saturated under 0.5 hour. In other words, a higher concentration was affected the efficiency of DSSC.

Yaguchi, Katoh, Murai, Watanabe, and Furube (2010) did the study of the various dye concentration. The absorbance of the film samples increased with increased dye solution, from 0.1 (0.01 mM) to 0.85 (0.05 mM). Besides, the adsorption spectra of N3 in solution shifts toward longer wavelengths with increased pH. This is because the coverage of dye on the TiO<sub>2</sub> surface was very low with lower pH. By increased the pH, there are presence of aggregation problem.

## 2.3 Nanocrystalline Oxide Semiconductors

Central to the DSSC device is a nanoparticle film that provides a large surface area for the adsorption of light harvesting molecules. Typically, the photoanode of the DSSC are constructed by wide band gap metal oxide film, such as  $\text{TiO}_2$ ,  $\text{ZnO}$ ,  $\text{Nb}_2\text{O}_5$  and other type binary oxide. Among all the oxides, the most effective is the  $\text{TiO}_2$  since it is widely available, non-toxic and gives promising performance of the cells.

### 2.3.1 Titanium Oxide ( $\text{TiO}_2$ )

Commonly, the  $\text{TiO}_2$  is used as the photoelectrodes since it has high porosity, high stability and wide band-gap energy. Typically, two structure of the  $\text{TiO}_2$  are involved in the DSSC; anatase and rutile phase. The anatase phase is commonly used as the active or first  $\text{TiO}_2$  layer while the rutile phase is used as the scattering layer.

One of the crucial aspects that determine the cell performance is the formulation of the nanocrystalline  $\text{TiO}_2$  paste since the overall energy conversion efficiency of the cell strongly depend on its surface and electronic properties. In the study of Dhungel and Park (2010), the optimized  $\text{TiO}_2$  paste was prepared by 26%  $\text{TiO}_2$  powder, 15% ethyl cellulose (EC), and 59%  $\alpha$ -terpineol. This is because this paste given conversion efficiency as high as 7.27%.

Dhungel and Park (2010) stated that a suitable ratio of the EC to  $\text{TiO}_2$  powder was found to be crucial to optimise the properties of the paste. As a binder, EC plays a critical role in optimising pastes containing a high solid loading because it affects the viscoelastic properties during the film casting as well as the properties such as the strength, density, and topological structure after sintering. Thus, it improved adhesion of the  $\text{TiO}_2$  power on the flouride tin oxide (FTO) glass surface.

Pastes with EC percentage higher than 15% than shown low efficiency and poor adhesion between TiO<sub>2</sub> film on the FTO glass surface due to the formation of excessively large void between the nanoparticles after the EC burns off. While pastes with EC percentage lower than 15% result crack on the films when drying, due to the reduced network strength of the paste. Thus, the optimised paste could be the solution in maintaining a balance between the mechanical, optical, and electrical properties of the TiO<sub>2</sub> film in the DSSC.

Another crucial aspect that determined cell performance is the particles size of the TiO<sub>2</sub>. Typically, the highest efficiency of the DSSC was prepared from the particles size between 20 to 30 nm. Generally, the diffusion coefficient of electron,  $D$  is proportional to the particles size, due to the lower number of the boundary among the particles. In the study of Mori and Yanagida (2006),  $D$  was increased with the particles size range from 14 to 41.5 nm. This is because most charge traps were located at the surface of the nanoporous semiconductor oxide with the large particles size.

However, in the view of charge recombination, the electron lifetime was inversely proportional to the  $D$ . Increased particles size may increased the  $D$  but it could decreased the electron lifetime as well. Thus, it promoted the charge recombination and lower efficiency result. In the study of Dhungel and Park (2010), optimum particles size of the active TiO<sub>2</sub> layer is 20 nm. This is because 20 nm have poor tendency to agglomerate and the lower recombination rate as compared to other particles size.

Dhungel and Park (2010) also did the study of XRD pattern. The recommend phase of the anatase structure TiO<sub>2</sub> as the single layer since it proven as the better candidate than rutile and brookite phases as the dye dispersed and adhered better to the TiO<sub>2</sub> particles surface. Besides, Satyen (2005) also did the XRD pattern study. This group found the surface area and adsorbed dyes on the rutile-TiO<sub>2</sub> was about 25% and 35% less than anatase-TiO<sub>2</sub>. According to Mori and Yanagida (2006), the standard anatase TiO<sub>2</sub> phase has 60% porosity, 50m<sup>2</sup> g<sup>-1</sup> surface area when the particles were 20 nm.

In the study of Yang et al. (2008), the cauliflower-like TiO<sub>2</sub> rough sphere, about 200 nm large, have greatly enhance light harvesting efficiency and energy conversion of the DSSC. 200 nm rough sphere TiO<sub>2</sub> was given better performance because it able to give scattering effect. Three experiments carried out by this group, which were rough sphere TiO<sub>2</sub> with 200 nm (RS), smooth sphere TiO<sub>2</sub> (SS) with 200 nm and normal particles size of 20 nm TiO<sub>2</sub>. As compare the result, the RS has the highest efficiency (6.56%) although the SS (5.43%) given higher average pore size. Thus, larger particles size able gives better scattering effect to improve the cell performance. However, the fabrication of this RS is different from the usual since it is synthesized from hydrolysis of Ti (OBU)<sub>4</sub> by using tri-block copolymer.

Another crucial aspect that determined cell performance efficiency is the thickness of the TiO<sub>2</sub>. In the study of Ito et al. (2007), the optimum film thickness for high efficient DSSC was 12-14 μm. This optimum thickness is based on the relationship of the electron diffusion length (L) with electron diffusion coefficient (D) and electron lifetime (τ). The L is square root of the product of the D and τ. In order to collect the most injection electron, the thickness must be at least of the L value. Film layer which less than 14 μm resulted low conversion efficiency due to increase of the D and film layer which larger than 14 μm tends to crack because of the film shrinkage.

According to Hore et al. (2006), the 4 μm thickness of the nanoporous TiO<sub>2</sub> film only given 3.2% ( $J_{sc}= 6.42$ ,  $V_{oc}= 0.71$ ,  $FF=0.70$ ) while 8 μm thick of the nanoporous TiO<sub>2</sub> film given 4.7% ( $J_{sc}= 9.17$ ,  $V_{oc}= 0.71$ ,  $FF=0.73$ ). This significant improvemet was concluded cause by the films thickness. As thickness of film increased, electron diffusion coefficient and the electron lifetime were higher. Thus the higher efficiency of the DSSC was obtained. This condition also observed in the study of Koo et al. (2007). According to Koo et. al, the 7μm thickness of the nanoporous TiO<sub>2</sub> film given  $7.55\pm 0.12\%$  ( $J_{sc}= 12.2\pm 0.1$ ,  $V_{oc}= 0.87\pm 2$ ,  $FF=0.71\pm 0.1$ ) while 14 μm thick of the nanoporous TiO<sub>2</sub> film given  $8.60\pm 0.08\%$  ( $J_{sc}= 15.2\pm 0.1$ ,  $V_{oc}= 0.81\pm 3$ ,  $FF=0.69$ ).

In the study of Koo et al. (2007), the dye-coated TiO<sub>2</sub> film in DSSC plays an important role in converted the photons to electrical energy since dyes generated photo-excited electrodes and the TiO<sub>2</sub> film serves as a pathway for photo-injected electrons. Increase surface area of the nanocrystalline TiO<sub>2</sub> able to gain more photos since high surface area able to increase the amount of adsorbed dye onto the TiO<sub>2</sub> electrode. However, it is restricted because the increase surface areas induce the recombination reaction. Besides, the wavelength of the film absorption becomes extended in the multilayer TiO<sub>2</sub> thin film as compare to the single layer TiO<sub>2</sub> thin film.

Scattering layer has been introduced for DSSC device in order to enhance cell performance without induced recombination. Hore et al. (2006) reported the used of transparent high surface area TiO<sub>2</sub> layer and an additional scattering layer which comprised of larger particles able ensured adequate light trapping in DSSC. Typically, the larger particles TiO<sub>2</sub> which may consist of the rutile phase is used as the scattering layer. The scattering effect of the larger TiO<sub>2</sub> particles enhances the photocurrent density and thereby overall conversion efficiency.

Three types of the scattering layer prepared by Hore et al. were commercial available powder of ZrO<sub>2</sub>, TiO<sub>2</sub>-rutile phase, and mixture of these two powders (ZrO<sub>2</sub> and TiO<sub>2</sub>-rutile phase). Among these three scattering layers, found that the mixture scattering layer has the highest efficiency, which is 6.8%. While efficiency for both ZrO<sub>2</sub> and TiO<sub>2</sub>-rutile phase scattering layers were only 5.8%. Mixture of scattering layer coated on the single TiO<sub>2</sub> layer was given significant scattering effect to increase the DSSC efficiency.

According to Koo et al. (2008), the scattering effect is dependent on size, refractive index and position of the scattering particles. Therefore, the relationship between the scattering effect and properties of the scattering particles are important to maximize the scattering efficiency. In the study of Koo et al. two type nanocrystalline TiO<sub>2</sub> single layers and the two kind particles sizes of scattering layer were investigated. Two type nanocrystalline anatase TiO<sub>2</sub> layer thickness were 7 μm (*1L*) and 14μm (*2L*). Two kind particles sizes for scattering layer were 0.3μm (*G1*) and 0.5μm (*G2*). Both of these two particles sizes were in rutile phase.



Efficiency of  $1L$ ,  $1L+G1$  and  $1L+G2$  was  $7.55\pm 0.12\%$ ,  $8.94\pm 0.08$  and  $8.78\pm 0.09\%$ , respectively. Efficiency of  $2L$ ,  $2L+G1$  and  $2L+G2$  was  $8.60\pm 0.08$ ,  $9.09\pm 0.09$  and  $9.15\pm 0.05$  respectively. Among these samples, found that the highest efficiency was achieved by  $2L + G2$  layer. Improved efficiency was mainly caused by the increase the photocurrent density which enhance by the scattering layer. However, the most increasing rate was the  $1L + G1$  layer where the increasing rate achieve  $+18.4\%$ . Film thickness is related to the wavelength of the transmitted light. From the result obtained, it is believed that the transmitted light passing through the thin nanocrystalline ( $1L$ ) layer is higher than the thick ( $2L$ ) nanocrystalline layer. Thus, the efficiency of the thin layer should be higher than the thick layer. However, as combine the  $1L + G2$ , the cell performance is lower than the  $1L + G1$ . This cause by the small scattering particles ( $G1$ ) exhibit better scattering efficiency since it has higher reflectance property in visible light.

Another scattering layer effect is stated by Ito et al., the double layer is term by a  $\text{TiO}_2$  films which consisted of transparent nanocrystalline (20 nm) and microcrystalline light-scattering anatase particles layer (400 nm). This double layer was used for DSSC photocurrent enhancement. Photovoltaic parameters performances without light-scattering layer present are  $J_{sc}= 15.6 \text{ mA/ cm}^2$ ,  $V_{oc}= 0.791 \text{ V}$ ,  $FF= 0.740$  and the efficiency,  $n= 9.12\%$  while upon addition of the light scattering layer. While the performance of double layers displayed an enhancement, there are  $J_{sc}= 18.2 \text{ mA/ cm}^2$ ,  $V_{oc}= 0.785 \text{ V}$ ,  $FF= 0.704$  and the efficiency,  $n= 10.1\%$ .

Besides, Ngamsinlapasathin, Srcethawong, Suziki, and Yoshikawa (2005) did the scattering layer research. The different scattering layer material was used for the scattering layer effect as same with the previous purpose. The double layers of this group was composed of a scattering layer (blended of MP- $\text{TiO}_2$  and P25 powder) that coated an active layer of mesoporous  $\text{TiO}_2$  (MP- $\text{TiO}_2$ ) film. According to Ngamsinlapasathin, et al. (2005), the  $\text{TiO}_2$  film tends to crack because of shrinkage if the film thickness was too thick.

The shrinkage resulted from the evaporation and deposition of the organic substance and the volume change owing to the crystallization induces considerable stress in the resultant film. To avoid this problem, Ngamsinlapasathin, et al. was added the titania powder (P25) into the titania gel (MP-TiO<sub>2</sub>) to prevent the film shrinkage. This group was investigated the different between single (only blended of MP-TiO<sub>2</sub> and P25 powder layer) and double layer of MP-TiO<sub>2</sub>/ P25. The large particles in P25 were consisted rutile and anatase phase while the MP-TiO<sub>2</sub> was consisted only the anatase phase. The MP-TiO<sub>2</sub> was used because the high anatase phase content and high surface area which could provide more facilitates electron transport. Besides, this MP-TiO<sub>2</sub> structure enables a very rapid and highly efficient interfacial electron transfer between the metal oxide and redox active species. The highest conversion efficiency obtained by this group was 8.1 % with the double layer.

According Dhungel and Park, sintering temperature of the TiO<sub>2</sub> film was an important parameter to achieve high efficiency. This is because the sintering process could guarantee good electrochemical bonding between nanoparticles for maximizing electron diffusion length and a larger surface area for maximising dye sensitization and light harvesting. The sintering effect was investigated by Chang et al. (2010), shown the SEM micrograph of film cross-section for the sample with and without sintering. From the SEM micrograph, the TiO<sub>2</sub> film layer was appeared more compact than that without undergoing the surface treatment at 400 °C. This is because the internal gas and voids of the film layer can only be eliminated after the sintering operation. Besides, the sintering operation which utilized the heat energy was to convert all the rutile crystalline phase into anatase phase. This process are increase the quantity of the TiO<sub>2</sub> nanoparticles in a unit area of film, thus enhanced the adsorptive capacity of the dye.

Mori and Yanagida (2006) stated the relationship between the sintering temperature and surface area is proportional. As sintering temperature increased, electron diffusion coefficient and the surface area were higher. Ngamsinlapasathian et al. state the relationship between the sintering temperature and surface area was inversely proportional. This statement was supported by the XRD pattern of the TiO<sub>2</sub> film. The main peaks of the TiO<sub>2</sub> film become sharper with increasing sintering temperature. These sharper main peaks indicated the increased in the crystalline size.

Besides, the SEM images also indicated the surface area and porosity of the TiO<sub>2</sub> film at various temperatures were inversely proportional to the sintering temperature. The surface area and porosity at 350°C was 110 m<sup>2</sup>/g and 53 % respectively which only 51 m<sup>2</sup>/g and 47 % at 500°C sintering temperature.

Another key factor enable for high efficiency was the charge recombination process between injected electrons and oxidised dyes. Recombination process must be much slower than the electron injection and electron transfer from the iodine ion into oxidised dyes (regeneration dyes) to accomplish effective charge separation. Charge recombination in the dye/TiO<sub>2</sub> system was caused by the direct injection occurs from the ligands of dye to TiO<sub>2</sub> film. Surface treatment such as TiCl<sub>4</sub> able to retard charge transfer from the conduction band to dye cation and triiodine, which called as prevent the recombination loss.

Ito et al. (2008) found that the two consecutive TiCl<sub>4</sub> treatments performed when prepared the TiO<sub>2</sub> photoanodes for DSSC increased the cell performance. One of these two consecutive TiCl<sub>4</sub> treatments was performed prior screen printing and another one was performed after the screen printing of TiO<sub>2</sub> films. The initial TiCl<sub>4</sub> treatment could be enhancing the bonding strength between the FTO substrate and the porous TiO<sub>2</sub> layer. First TiCl<sub>4</sub> treatment can block the charge recombination between the electron emanating from the FTO and the triiodine ions presented in the redox couple. Second TiCl<sub>4</sub> treatment used to enhance surface roughness factor and necking of the TiO<sub>2</sub> particles thus better for dye adsorption.

This two consecutive TiCl<sub>4</sub> treatments resulted higher photocurrent and higher cell efficiency. Efficiency of DSSC without TiCl<sub>4</sub> treatment was 9.4% ( $J_{sc}$ = 16.6 mA/ cm<sup>2</sup>,  $V_{oc}$ = 0.778 V,  $FF$ = 0.731) while the efficiency of DSSC with two consecutive TiCl<sub>4</sub> treatments and scattering layer was 10.1% ( $J_{sc}$ = 18.2 mA/ cm<sup>2</sup>,  $V_{oc}$ = 0.789 V,  $FF$ = 0.704). Besides, efficiency of DSSC without light scattering layer was only 9.12% ( $J_{sc}$ = 15.6 mA/ cm<sup>2</sup>,  $V_{oc}$ = 0.791 V,  $FF$ = 0.740). As compare the result, found that the standard TiO<sub>2</sub> DSSC (with TiCl<sub>4</sub> treatment and light scattering layer) has given highest efficiency. Thus, it is believed TiCl<sub>4</sub> treatment able given significant effect on the efficiency of DSSC than light scattering layer.

According to Chou, Lin, Yang, and Liu (2011), the deposited a film of  $\text{TiO}_2/\text{NiO}$  composite particles can act as barrier for electron recombination. Thus, higher cell efficiency able obtained. Due to the mass ration of the  $\text{TiO}_2$  to Ni and the dry mixing method, the Ni powder could hardly be coated onto the entire surface of the  $\text{TiO}_2$  particles to create the prefect core-shell  $\text{TiO}_2/\text{NiO}$  composite particles. Therefore, after soaked the working electrode with  $\text{TiO}_2/\text{NiO}$  composite particles in the dye solution and ethyl alcohol, the dye able adhered to either the surface of the  $\text{TiO}_2$  particles or the surface of the NiO powder. Since the LUMO of the N719 dye (-0.70 eV) was below the conduction band (CB) of NiO (-2.36 eV), so it must energised much more electrons in order to pass through the CB of NiO. Then, the electrons were just able injected to the CB of  $\text{TiO}_2$ . Therefore, the NiO which adhered to the surface of  $\text{TiO}_2$  particles could act as a barrier for the electron recombination which leading to higher power conversion efficiency DSSC.

## **CHAPTER 3**

### **METHODOLOGY**

#### **3.1 Introduction**

Research and planning are the first step in the project before sample preparation and data collection. Research is done by studying the related articles, references, and some information from the internet. Reading and understanding all the articles give a better understanding about the project and create a better visualization in planning the steps to carry out the project. Thus chapter 3 for methodology will discuss mainly topic about:

- Raw materials and apparatus
- DSSC preparation and fabrication
- Equipments

#### **3.2 Raw Materials and Apparatus**

The raw materials required for a DSSC are wide band gap metal oxide, dyes, two piece transparent conductive glasses, and electrolyte. Following table represent the detail of the raw materials use in this project.

**Table 3.1: Introduction of raw materials for DSSC**

<b>Raw materials</b>	<b>Description</b>
<b>1. Titanium oxide (TiO<sub>2</sub>) paste</b>	Anatase nanoparticles TiO <sub>2</sub> paste with average particles size of 20 nm.
<b>2. Dyes/sensitisers</b>	There are two Ru complexes dye used in this project which were N3 dye and N719 sensitiser. Both of these sensitisers were in crystalline form. Thus, these sensitisers need dilute with pure ethanol.
<b>3. Electrolyte</b>	Electrolyte used in this project was ionic liquid which the composition is 0.6 M BM II, 0.03 M I <sub>2</sub> , 0.10 M guanidinium thiocyanate and 0.5 M 4-tert-butylpyridine in a mixture of acetonitrile and voleronitrile (volume ratio, 85:15).
<b>4. Transparent conductive glass</b>	Transparent conductive glass plate which the conducting layer is the FTO. The sheet resistance of the conductive coating is approximately 15 Ω/sq.
<b>5. Platinum (Pt) coated glass plate</b>	Platinum (Pt) coated glass plate as the counter electrode. The dimension of this Pt counter electrode is 160 mm*80 mm*3.2 mm.
<b>6. Sealant</b>	The film thickness of this thermoplastics sealant is 30 μm.

<p><b>7. Cleaning Solutions</b></p> <ul style="list-style-type: none"> <li>• Deionized water</li> <li>• Absolute ethanol (99.8%)</li> <li>• Acetone</li> </ul>	<p>Use to remove the contaminants at the surface of the FTO.</p>
--	--

While for the apparatus which needed are:

**Table 3.2: Apparatus**

Scotch tape	Beaker	Spatula	Vacuum pump	Diamond cutter
Microbalance	Bottles	Cotton buds	Hotplate	Aluminium foil
Forceps	Gloves	Facemask	Parafilm	Measuring cylinder

### 3.3 DSSC Preparation and Fabrication

Normally, there are five general steps for fabrication of a DSSC, which are preparation of photo-electrode, preparation of counter electrode, physical assembly, electrolyte preparation, and final cell assembly. Scheme 3.1 describes the overall process for fabrication of the DSSC in this project.

Before the start of any procedure in the fabrication of DSSC, the dyes need to be diluted with the ethanol solution first since the dyes are in crystalline form. This step was carried out to ensure the smoothly of the processing. The first step in the fabrication of DSSC was prepared FTO glass and Pt-counter electrode glass preparation. There were include tested the conductivity of the FTO glass, cut the FTO glass and Pt-counter electrode glass by diamond cutter, cleaned and rinsed with ethanol, acetone, deionised water in order to remove the contaminants.

Following step was applied the  $\text{TiO}_2$  paste on the FTO conductive surface by doctor blade techniques. Double layer of the 20 nm particles size  $\text{TiO}_2$  is fixed in this work in order to investigate the sensitizer effect to the efficiency. A doctor blade technique is the technique where a smooth glass rod is manually spreads a viscous colloide on a FTO glass surface to a specific thickness with help of a tape frame. This step was repeated twice in order to achieve the require thickness. Then FTO /  $\text{TiO}_2$  layer was obtained. Then, FTO /  $\text{TiO}_2$  layer was sent for sintered at around  $450^\circ\text{C}$  to remove the organic solvent in hotplate. After this, FTO /  $\text{TiO}_2$  which obtained just now were soaked into the dye solution and then coated it with Al foil in order to avoid evaporation. After the step, FTO /  $\text{TiO}_2$  / Dye layer which call photoelectrode was obtained.

After that, the following procedure was drilled a hole at the counter electrode before seal the photoelectrode and counter electrode with hot-melt gasket. Finally, electrolytes were added through the hole in the back of the counter electrode. After the DSSC was fabricated, the following was sent the cell for measured the performance under suitable device which discussed later.



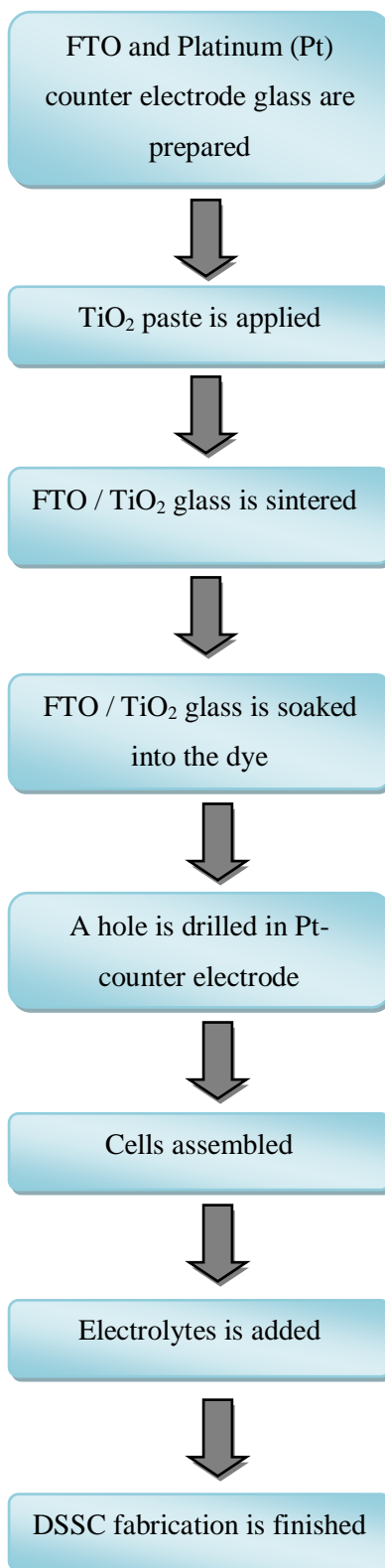


**Figure 3.1: Process flow chart for fabrication of DSSC**

### 3.4 Equipment

Several equipment for the DSSC were available for this project, which are I-V Tester, UV (ultra-violet) Visible Spectrophotometer, X-ray diffraction (XRD), and Scanning Electron Microscope (SEM).

#### 3.4.1 Current-Voltage (I-V) Tester

Figure 3.1 shows the I-V Tester used to run current-voltage measurement and determine the critical parameter such as short circuit current ( $I_{sc}$ ), current density ( $J_{sc}$ ), open circuit voltage ( $V_{oc}$ ), fill factor ( $ff$ ), maximum output power ( $P_{max}$ ), cell efficiency ( $\eta$ ) and other standard photovoltaic cell parameters. The station can include a source meter, reference cell, cell holder, probing assembly, measurement software depending upon the configuration required. I-V characteristics of DSSC were identifying by applies the bias externally and measuring the generated photocurrent by using a Lab-view based I-V measurement software. The applied bias range from -0.1 V to 0.8 V.

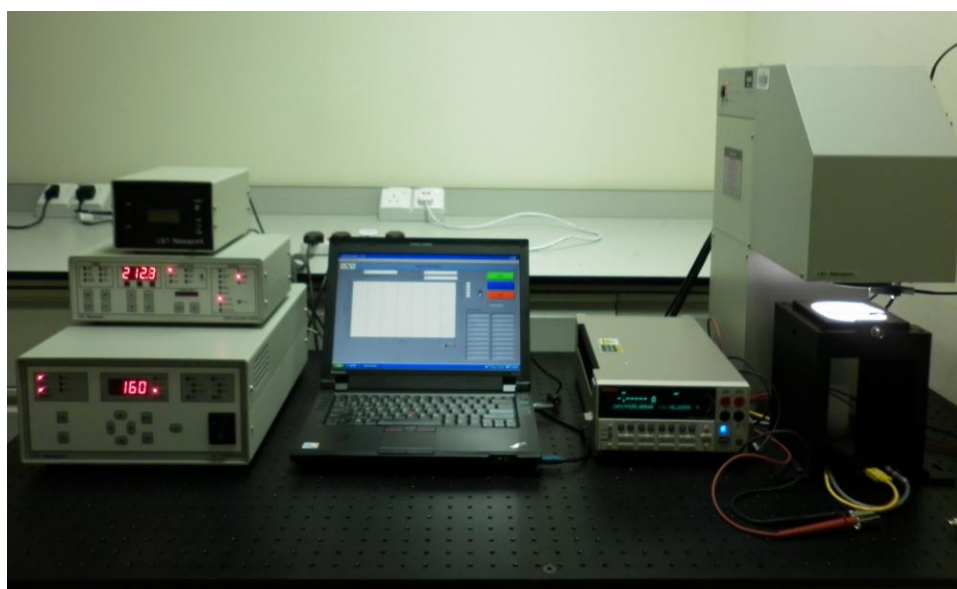


Figure 3.2: IV-tester

### 3.4.2 UV (Ultra-Violet) Visible Spectrophotometer

Figure 3.2 shown the UV (Ultra-Violet) Visible Spectrophotometer used to measures the intensity of light passing through a sample ( $I$ ), and compared it to the intensity of light before it passes through the sample ( $I_0$ ). The ratio of the  $I / I_0$  is term as transmittance, and is usually expressed as a percentage (%). The absorbance was based on the transmittance. Besides, it can also explain as an outstanding method that used for quantitative of the substances that absorb in the ultraviolet-visible spectral region. Means that it could used to determine the absorbance of the substances ( $\text{TiO}_2$  film with sensitized with dye) over the wavelength of visible and adjacent (near-UV and near-infrared (NIR)) ranges. Usually, the graph obtained by this measuring testing system was the absorbance versus wavelength.



Figure 3.3: UV (Ultra-Violet) Visible Spectrophotometer

### 3.4.3 X-ray diffraction (XRD)

Figure 3.3 shows the Shimadzu XRD 6000 used for the crystallographic studies of materials. The XRD model available in Universiti Tunku Abdul Rahman (UTAR) is the Shimadzu XRD 6000. This instrument offers solution comprising wide-ranging analysis requirements, from routine qualitative and quantitative analysis to state change analysis, including crystalline size / lattice strain, crystalline calculate, materials analysis via overlaid X-ray diffraction patterns, enhanced material evaluation, and sample heating analysis. In this project, the Cu K-alpha radiation x-ray with the wavelength of  $\lambda=1.5406 \text{ \AA}$  operating at 40 kV and 40 mA is used as the incident beam. The sample was tilted  $0.5^\circ$  towards the x-ray beam and fixed throughout the 2-theta detector scan from  $20^\circ$ -  $80^\circ$  range with a scan rate of  $2^\circ$  per minute.



Figure 3.4:X-ray diffraction (XRD)

### 3.4.4 Scanning Electron Microscope (SEM) and Energy Dispersive Spectroscopy (EDS)

Figure 3.4 shows Scanning Electron Microscope (SEM) and Energy Dispersive Spectroscopy (EDS). In this project, a Hitachi S-3400N SEM was used to examine the surface structures with nanometer (nm) spatial resolution. It used for the morphology studies of the materials. From the micrographs, it was able to observe that whether the uniform and homogenous distribute of the dye on the TiO<sub>2</sub> electrode surface and cross section or creak initial in the thin film. Furthermore, EDS able indentified the chemical composition and weight ratio of the sample. EDS is a chemical microanalysis technique used in conjunction with SEM. EDS technique detected x-rays emitted from the sample during bombardment by an electron beam to characterise the elemental composition of the analyzed volume. However, lower resolution of this SEM given relatively poor quality images.

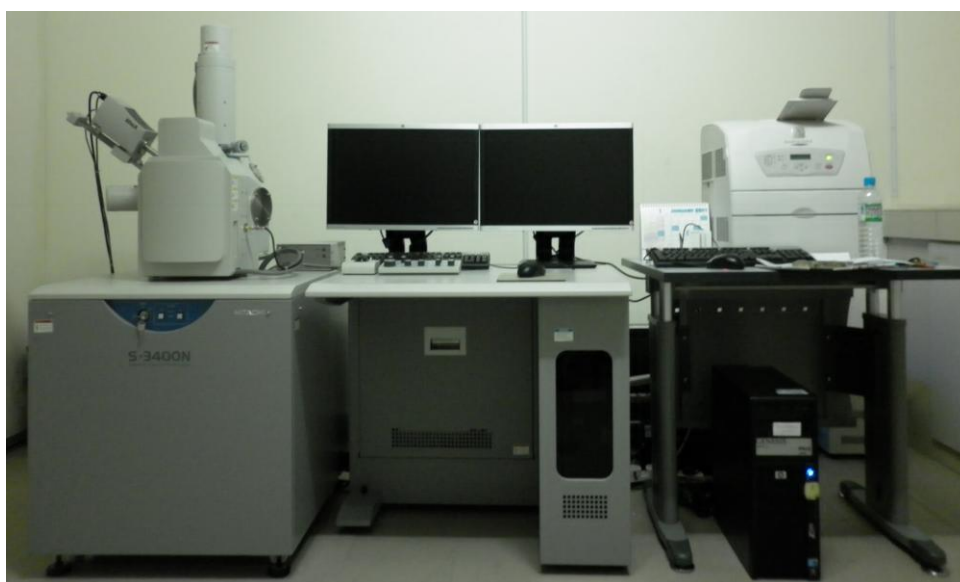


Figure 3.5: Scanning Electron Microscope (SEM) and Energy Dispersive Spectroscopy (EDS)

## CHAPTER 4

### RESULTS AND DISCUSSION

#### 4.1 Characterisation of DSSC with different Dye/Sensitiser

##### 4.1.1 I-V Test

The current-voltage curves obtained from I-V Tester can be used to evaluate the photovoltaic performance of DSSC with different sensitisers. Figure 4.1 shows the comparison of the I-V characteristic between two sensitisers, N3 and N719.

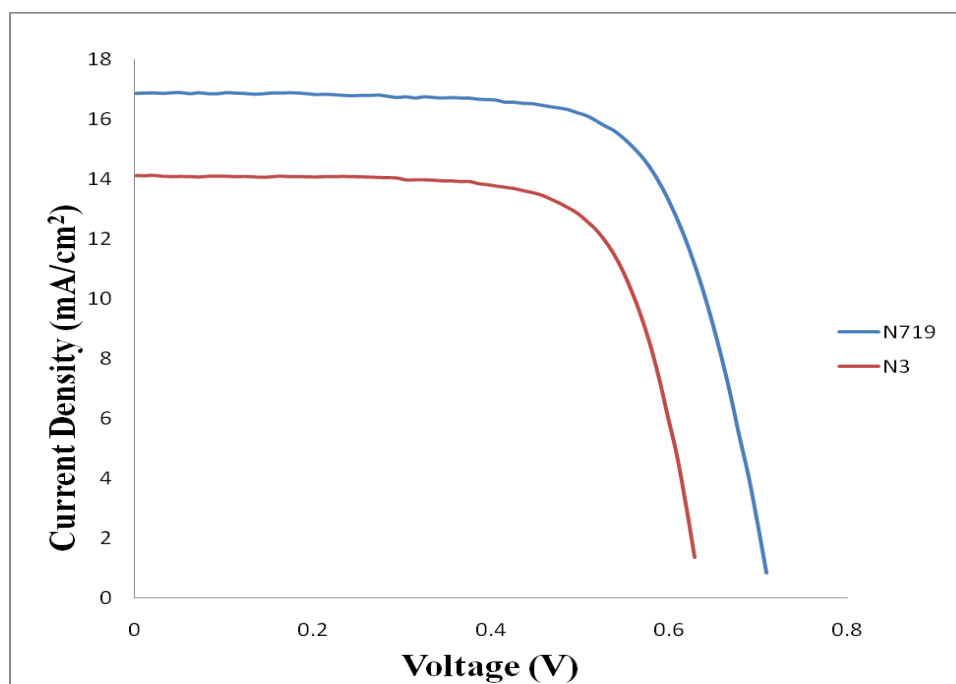


Figure 4.1: Current-to-voltage curve with N3 and N719 sensitisers.

**Table 4.1:** Photovoltaic characteristic for different sensitiser, N3 and N719

Types of dyes	Efficiency, $\eta$ (%)	Fill factor, FF	Open circuit voltage, $V_{oc}$ (V)	Current density, $J_{sc}$ (mA/cm <sup>2</sup> )
N719	8.43	0.70	0.71	16.89
N3	6.58	0.71	0.63	14.51

Refer to the Figure 4.1 and Table 4.1, it is clearly seen that the N719 gives a better photovoltaic performance (8.43%), a much higher efficiency than N3. Results curve can refer to Appendix D. The efficiency is expressed by following equation:

$$\eta = \frac{V_{oc} * I_{sc} * FF}{P_{in}} \times 100\% \quad (4.1)$$

where

$FF$  = Fill factor

$I_{sc}$  = Short circuit current, mA

$V_{oc}$  = Open circuit voltage, V

$P_{in}$  = Solar radiation intensity

Equation 4.1 shows that  $\eta$  of the DSSC depends on few parameters, such as  $V_{oc}$ ,  $I_{sc}$ , and  $FF$ . This means that to improve the efficiency of the DSSC, it is necessary to increase the  $V_{oc}$ ,  $I_{sc}$ , and  $FF$  since there is proportional to the  $\eta$ .  $J_{sc}$  (mA/cm<sup>2</sup>) refers to the ratio of the current to the active area. Hence, higher  $J_{sc}$  result higher efficiency.

Compare the molecules structures (refer Appendix A of the two sensitiser), they are identical with the only difference in the degree of protonation. N3 sensitiser has four carboxylate groups in its structure while N719 only two, with the two protons ( $H^+$ ) in the carboxylate group is substitute by a tetra butylammonium cation ( $TBA^+$ ) group. By replace this  $TBA^+$  group, higher  $V_{oc}$  (0.71 V) deliver by N719 sensitiser than N3 sensitiser (0.63 V). This  $TBA^+$  group cause a modest energy down-shift on the  $TiO_2$  conduction band because these  $TBA^+$  group are stand away

from the nanoporous oxide semiconductor surface. Thus, it is believed DSSC with N719 sensitizer gives higher efficiency than N3. Besides, Thavasi et al. found that the fully protonated N3 sensitizer possessed an excellent light-harvesting property but poor electron injection efficiency due to the misalignment of the dye N3 on TiO<sub>2</sub>. For the N719 sensitizer, the misalignment problem does not occur. Thus, N719 shows higher electron injection, indicated by the  $J_{sc}$ .

When the sensitizer is chemically bound to the TiO<sub>2</sub>, the protons of the anchoring group (carboxylic group) are partly transferred to the surface of TiO<sub>2</sub>. Thus, another consequence of TBA<sup>+</sup> substitution is a higher driving force for charge injection to conduction band of TiO<sub>2</sub>, which increases the  $I_{sc}$  and hence the  $J_{sc}$ . In other words, the electron transport from N719 to conduction band of TiO<sub>2</sub> is much faster than N3. It is observed from this work, the  $I_{sc}$  and  $J_{sc}$  of N719 is much higher than the N3.

In addition, N719 sensitizer has a lesser number of COOH groups and it could exhibit lesser or no agglomerations on metal oxide surface compared to N3. This aggregation may occur via the intermolecular hydrogen bonding. This coordination is unfavourable as the dye molecules are not in close proximity to TiO<sub>2</sub> and hence cannot electrically bind to TiO<sub>2</sub> (Lee, 2010). Therefore, the injection rate of the aggregate dye to metal oxide is much slower. Hence lowering the  $J_{sc}$  of the N3. With the increase of  $J_{sc}$ ,  $V_{oc}$  and  $FF$  as explained above, the efficiency of DSSC with N719 sensitizer is proven higher than N3.

In the study of Jang et al. (2007), the efficiency of the DSSC with N3 sensitizer is 5.7%, lower than that obtained in this project (6.58%). It is believed that the difference is due to the concentration of the dye solution. The concentration of the N3 dye solution used by Jang and his co-workers is 0.5 mM while only 0.3 mM is used in this project. According to Katoh, Fuke, Furube, and Koide (2010), higher concentration might cause the dye aggregation in solution due to the solubility of the fully protonated N3 sensitizer is not high. Thus, DSSC with lower dye solution's concentration would possess a higher efficiency due to less aggregation problem.



Ito et al. (2008) studies the efficiency of DSSC with N719 sensitiser, treated with  $\text{TiCl}_4$  solution and sintered at  $500^\circ\text{C}$  produced the DSSC which used N719 as sensitizer almost similar with this work. In this study, DSSC is sintered at  $450^\circ\text{C}$  and without  $\text{TiCl}_4$  treatment. The efficiency obtained was 9.12% higher than that of this study (8.43%), probably because of the difference in those two factors. According to Ito et al.(2008), surface treatment able to retard charge transfer from the conduction band to dye cation and triiodide, preventing the recombination loss. Besides,  $\text{TiCl}_4$  treatments also increase the rough factor. Augmentation in the roughness factor leads to increase in the absorbance. Thus, more dye molecules able absorbed and higher efficiency obtained.

According to Ngamsinlapasathian et al. (2005), increase in sintering temperature decreased the amount of adsorbed dye onto the metal oxide surface; Kantonis, Stergiopoulos, Katsoulidis, Pomonis, and Falaras (2011) suggested that the lowest sintering temperature should be  $400^\circ$  while the sintering temperature is limited up to  $550^\circ$ . This means sintering temperature used in this project is within the suitable temperature range and not affect the performance of DSSC. Therefore,  $\text{TiCl}_4$  treatment and sintering temperature not as a factors that causes the lower efficiency of DSSC in current study.

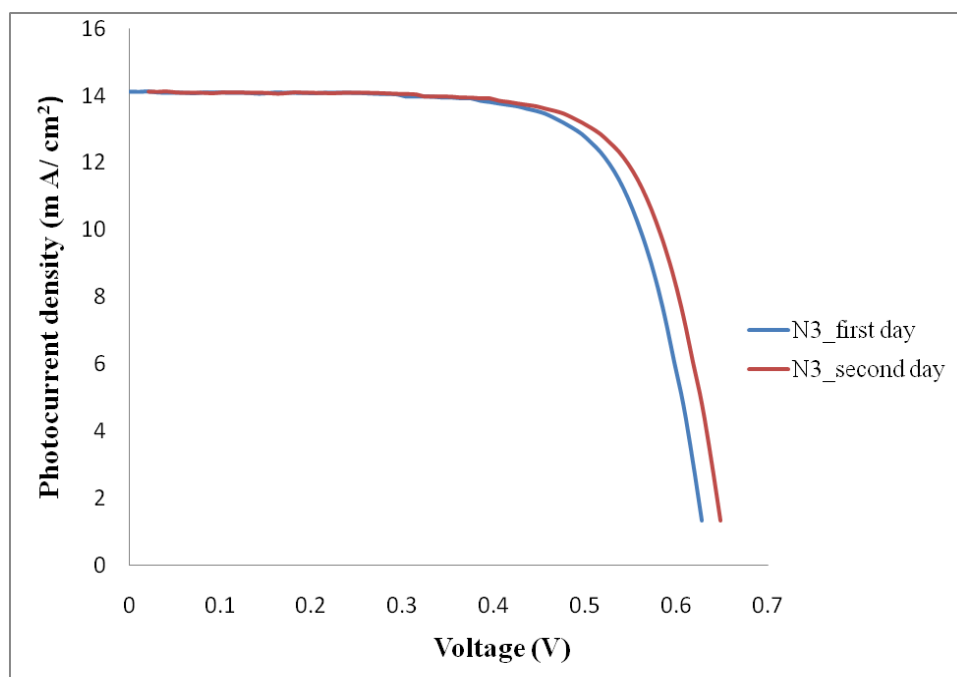


Figure 4.2: I-V curve with N3 for first and second day measurement

**Table 4.2:** Photovoltaic characteristic of N3 for first and second day measurement

Day of Measurement	Efficiency, $\eta$ (%)	Fill factor, FF	Open circuit voltage, Voc (V)	Current density, Jsc (mA/cm <sup>2</sup> )
First day (blue)	5.83	0.67	0.65	13.11
Second day (red)	6.58	0.71	0.63	14.51

The DSSC photovoltaic performance values for the DSSC with N3 sensitiser in first and second day measurement are different. The differences are indicated by Figure 4.2 and Table 4.2. The photovoltaic performance of N3 is better for the second day measurement. The efficiency in second day increases by 0.75%, the FF and  $J_{sc}$  increases by 0.04 and 1.4, respectively in comparison with the first day measurement. This increment is due to the longer time provided for the electrolyte to penetrate into the TiO<sub>2</sub> pores. This view is supported by the Seo et al. (2010). Similar result is obtained in DSSC with N719 as shown in Figure 4.3 and Table 4.3.

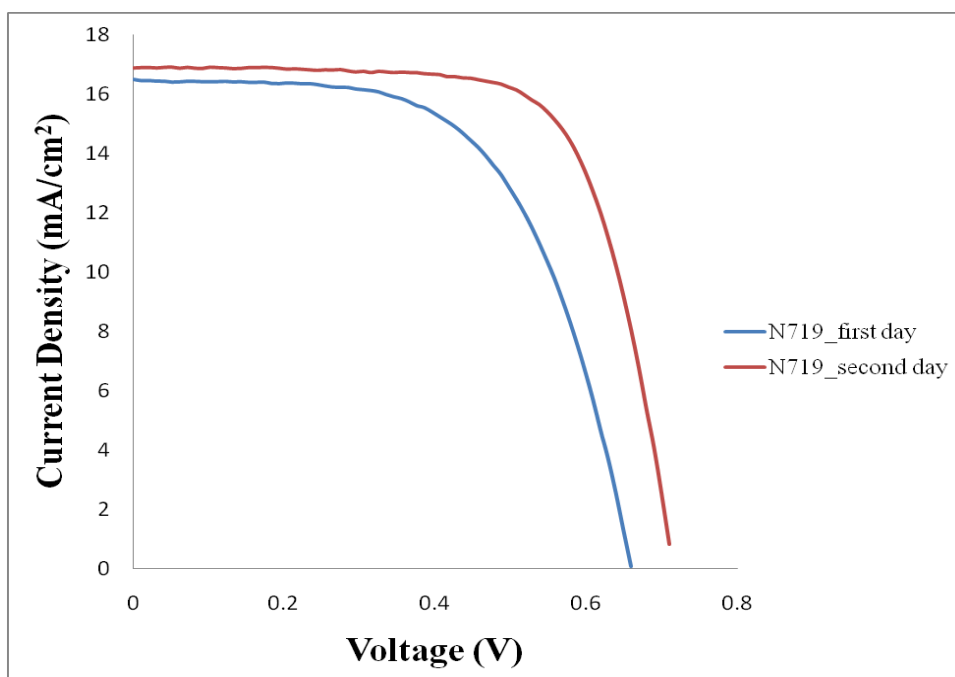


Figure 4.3: I-V curve with N719 for first and second day measurement

**Table 4.3:** Photovoltaic characteristic of N719 for first and second day measurement

Day of Measurement	Efficiency, $\eta$ (%)	Fill factor, FF	Open circuit voltage, Voc (V)	Current density, Jsc ( $\text{mA}/\text{cm}^2$ )
First day (blue)	6.50	0.60	0.65	16.44
Second day (red)	8.43	0.70	0.71	16.89

Based on the Figure 4.3 and Table 4.3, the photovoltaic performance of N719 is better for second day measurement. However, a large increment (1.93%) is seen in N719 cause by better performance of  $\text{TiO}_2/\text{N719}$  dye interface. The  $\text{TBA}^+$  group in N719 structure promote more electron injection to the  $\text{TiO}_2$ .

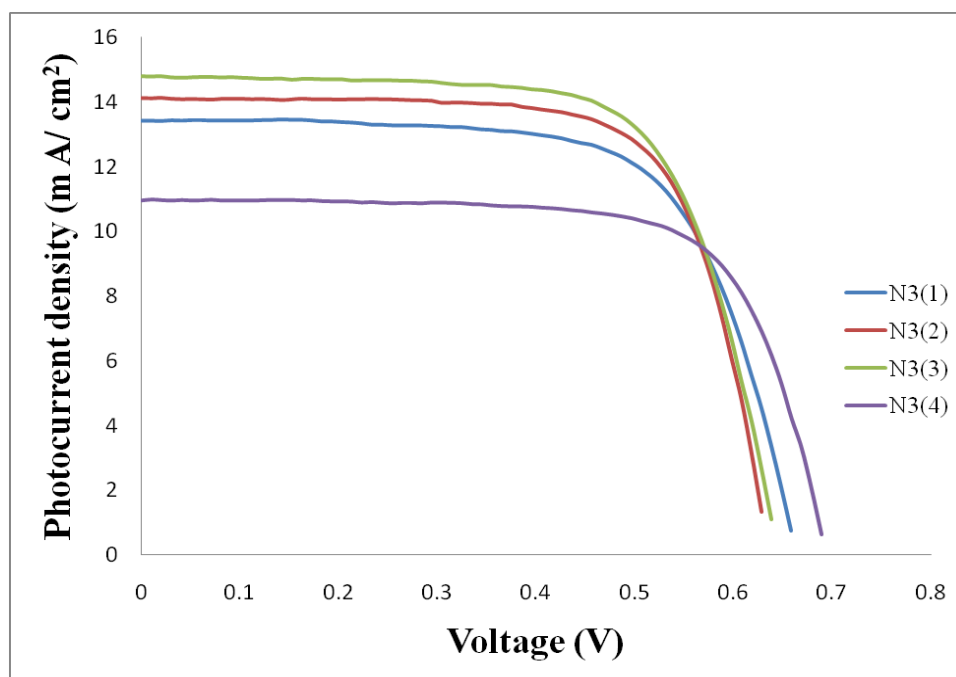


Figure 4.4: I-V characteristic of different DSSC with N3

**Table 4.4:** Photovoltaic performance of different DSSC with N3

DSSC Number	Efficiency, $\eta$ (%)	Fill factor, FF	Open circuit voltage, $V_{oc}$ (V)	Current density, $J_{sc}$ (mA/cm <sup>2</sup> )
N3(1)	6.04	0.68	0.66	13.42
N3(2)	6.58	0.71	0.63	14.51
N3(3)	6.61	0.70	0.64	14.77
N3(4)	5.42	0.71	0.69	11.00

In this study, four different DSSC with N3 dye has been tested for their photovoltaic performances. Results are summarised in Figure 4.4 and Table 4.4;  $\eta$ ,  $FF$ ,  $J_{sc}$ ,  $V_{oc}$  varies for each sample. This is probably because of the inconsistency  $TiO_2$  thickness as well as the uneven surface of the  $TiO_2$  film produced by the doctor blade's method. The thicker the  $TiO_2$  film, the more likely shrinkage would occur during the sintering process, resulting crack of the film while uneven surface would result in bad electron transport path. Therefore, the photovoltaic performance for every DSSC is not consistent. SEM micrographs are showed proven for this view.

#### 4.1.2 Morphology and Composition Studies

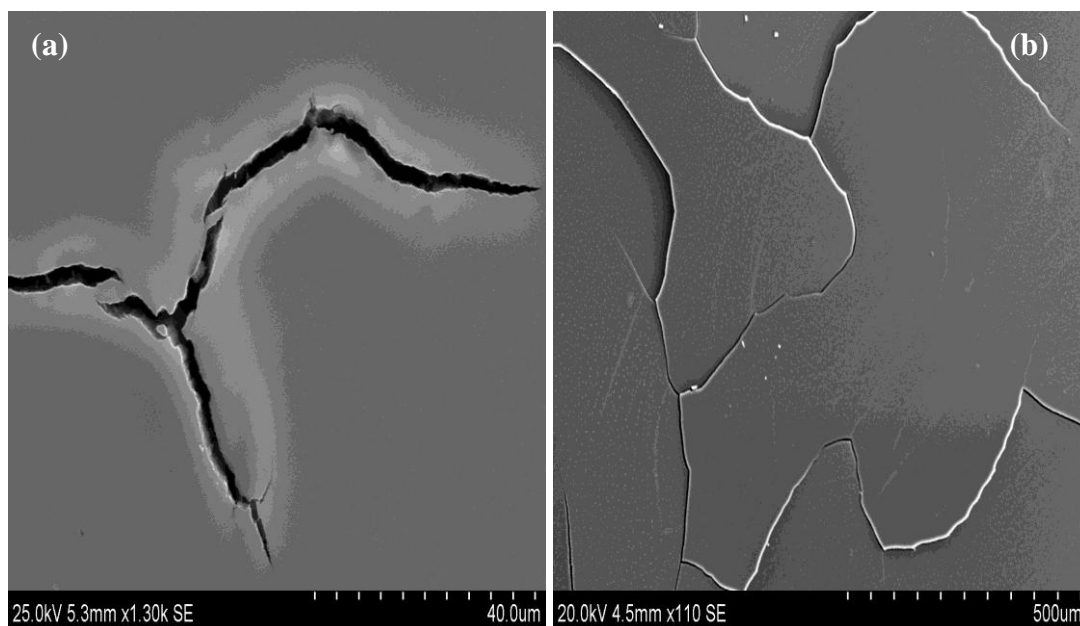
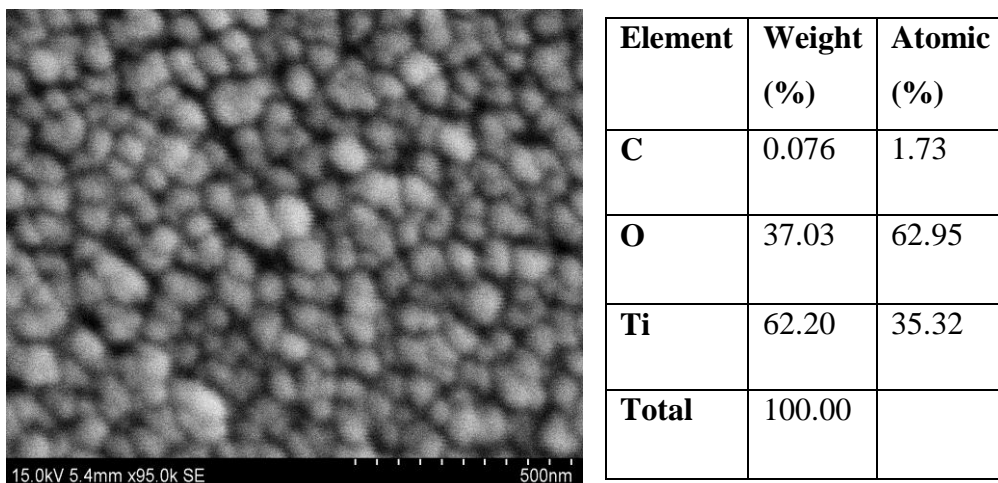
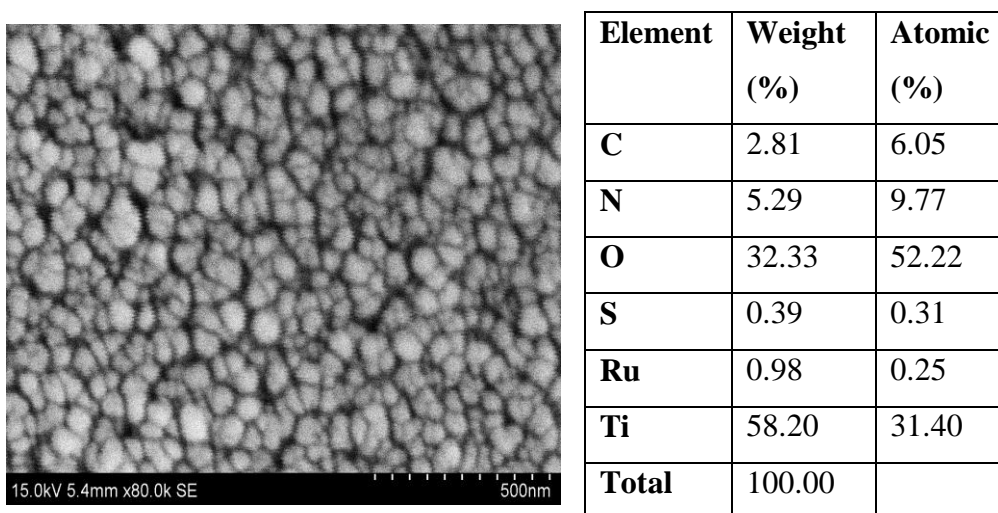
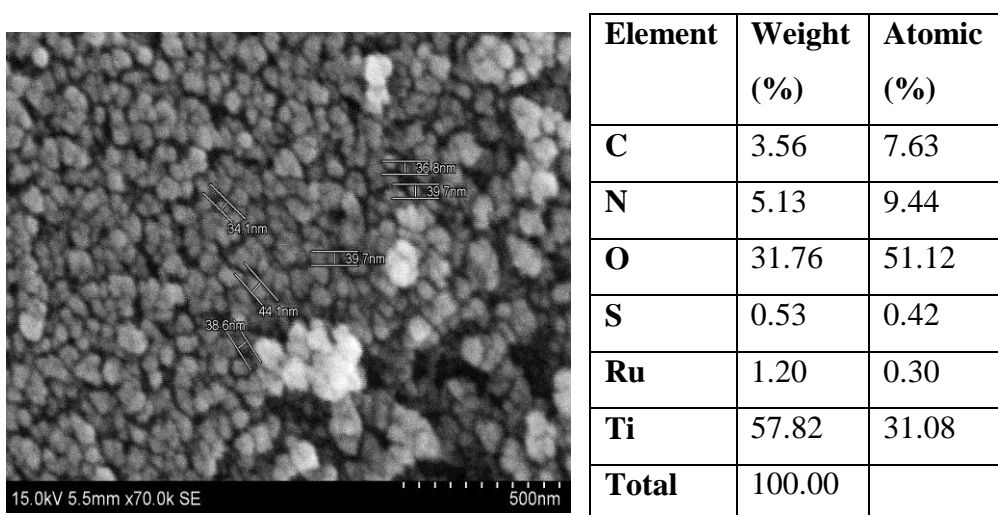


Figure 4.5: SEM micrographs of TiO<sub>2</sub> film (a) 1300X magnification (b)110X magnification

Figure 4.5 (a) and (b) show that there are many cracks on the surface of the TiO<sub>2</sub> thin films. Those cracks are formed before sintering and cannot be improved by sintering. In this study, doctor blade method is used to apply the TiO<sub>2</sub> paste on the FTO glass, inconsistency in the applied force/ thickness of the film, is likely to cause on the films; think (optimum thickness of 14-18  $\mu\text{m}$ ) TiO<sub>2</sub> films will likely to shrink during the sintering. The cracks would greatly affect the uniformity of the film and result in bad electron transport path. This view is supported by Dhungel and Park (2010).

Cracks on the FTO film have two negative effects on the DSSC's efficiency. Firstly, the adherence of TiO<sub>2</sub> thin film on the FTO surface is reduced causes difficulty in the DSSC assembly. Secondly, functional group of the N719 and N3 are carboxylate (COOH) has to conjugate with the hydroxyl (-OH) group of the TiO<sub>2</sub>, to enable the efficient transference of electrons to the nanoporous oxide semiconductor film. According to Chang et al. (2009), dye molecules that trap in cracks unable to do so and will be lost in the electrolyte. Hence, lower the  $J_{sc}$  and efficiency of the DSSC.

Figure 4.6: SEM micrograph and EDS data for 20 nm TiO<sub>2</sub> filmFigure 4.7: SEM micrograph and EDS data for 20 nm N<sub>3</sub>/TiO<sub>2</sub> filmFigure 4.8: SEM micrograph and EDS data for 20 nm N719/ TiO<sub>2</sub> film

SEM micrographs in Figure 4.6, Figure 4.7 and Figure 4.8 indicate that the samples are relatively porous and the  $\text{TiO}_2$  nanoparticles are homogeneously distributed. The dye molecules adsorbed on the  $\text{TiO}_2$  film surface cannot be resolved even using SEM technique because the size of the dye molecules is out of the measurement limitation. Therefore, the morphologies of those three samples do not show much difference. Besides, dyes are organic and non-conductive. Consequently it is difficult to view by SEM. This view is supported by Kim et al. (2010). Thus, EDS is performed to ensure the adherence of the dye molecules on the  $\text{TiO}_2$  surface (refer appendix F).

Ruthenium, Ru and sulphur, S elements are only detected in the samples soaking in the N3 and N719 dye solution. This proves the presence of the dye molecules in the N3/ $\text{TiO}_2$  and N719/ $\text{TiO}_2$  samples. Carbon, C element is detected on all samples probably due to the carbon tape used for the attachment of the sample to the holder, finger prints and also contaminates in the air.

EDS data in Figure 4.7 and 4.8, show that the weight ratio (%) Rus for N719 on the surface of the  $\text{TiO}_2$  is 1.73%, while 1.37% for the N3. This is probably attribute to the fact the dye coverage by the N719 is better than N3 under the same immersion or soaking condition (24 hours). Higher dye coverage in the N719 mean that the higher possibility of the electron injection to the  $\text{TiO}_2$  conduction band, leads to higher  $I_{sc}$  and  $J_{sc}$  and efficiency of the DSSC. This view is support by Chou et al. (2010).

### 4.1.3 X-Ray Diffraction Study

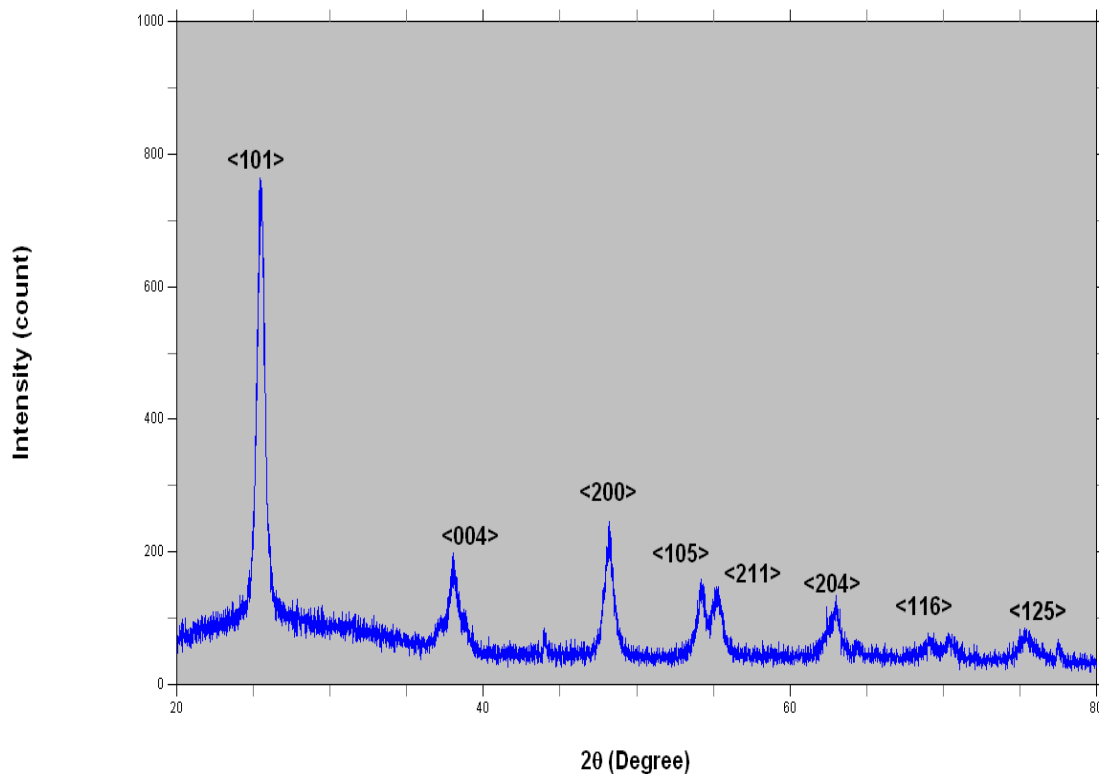


Figure 4.9: X-ray diffractogram of TiO<sub>2</sub> film

XRD is performed on the TiO<sub>2</sub> film to determine its phase identify and purity. Figure 4.9 show x-ray diffraction patterns of TiO<sub>2</sub> with the prominent peaks at the  $2\theta$  values of 25.40°, 38.03°, 48.09°, 54.18°, 55.09°, 62.83°, 69.10°, 75.27°, corresponding to diffraction from <101>, <004>, <200>, <105>, <211>, <204>, <116> and <125> planes, respectively. The XRD peaks with high intensity, suggesting that the TiO<sub>2</sub> particles are of high crystallinity. Cell refinement is performed using “CHEKCELL” and all the peaks could be fully identify as Thragonal with anatase structure, confirming the formation of phase compound, similar result is obtained by Yang et al. (2008) (refer appendix C).

Among all the polymorphs, the anatase structure shows the highest power conversion efficiency due to its small size and high surface area for optimum dye adsorption. Electron transport in the anatase TiO<sub>2</sub> is faster than that of rutile TiO<sub>2</sub>. This view is supported by Lee (2010), Satyen (2005), and Wong et al. (2004).



In addition, peaks for other phases such as rutile and brookite are evidently absent from the XRD result which indicate this sample is composed of anatase particles. Thus, comparable efficiency obtained by this work. However, some relative low intensity peaks of the anatase TiO<sub>2</sub> film are observed. This means small amount of the solvent are still contained in the film and does not totally evaporated through the 450°C sintered temperature.

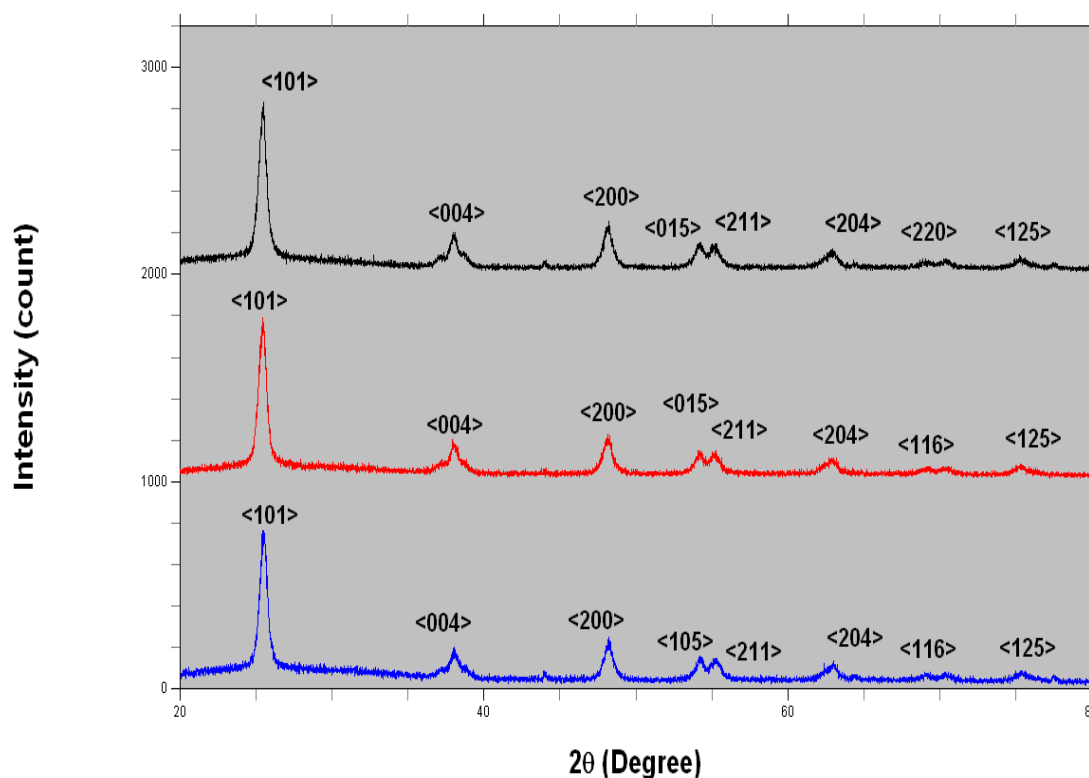


Figure 4.10: X-ray diffractogram of TiO<sub>2</sub> (Blue line), N3/TiO<sub>2</sub> (blue line) and N719/TiO<sub>2</sub> (black line)

Figure 4.10 compares the x-ray diffraction patterns of pure TiO<sub>2</sub> film, N3 coated TiO<sub>2</sub> film and also N719 coated TiO<sub>2</sub> film. The three x-ray diffraction patterns show no difference in the diffraction planes. This is because the dye molecules not only form a monolayer on the TiO<sub>2</sub> surface, it also experience the trap filling effect; the grain boundary or porosity or trap sites of the nanocrystalline TiO<sub>2</sub> are served as surface imperfections that separate grains of different orientation. In other words, those trap site/ grain boundary/porosity produce higher energy than the grain interior and cause the grain boundary more susceptible to fill with the dye molecules.

Therefore, it is difficult to get the peaks of the Ru complex dyes. Besides, the intensity of the Ru dyes peaks might be too low. This view is supported by Dittrich, Ofir, Tirosh, Grinis, and Zaban (2006).

#### 4.1.4 Dye Loading

A 99.8% pure ethanol was used as the solvent for the preparation of dye solution in this study due to few reason. According to Tannia Marinado (2009), the absorbance dye molecules for ethanol solvent is much higher than that of acetronitrile solution (refer Appedix B). Besides, Uam et al. (2010) found that the  $J_{sc}$  of the DSSC with acetronitrile solution decreases after 4 hour of illumination.

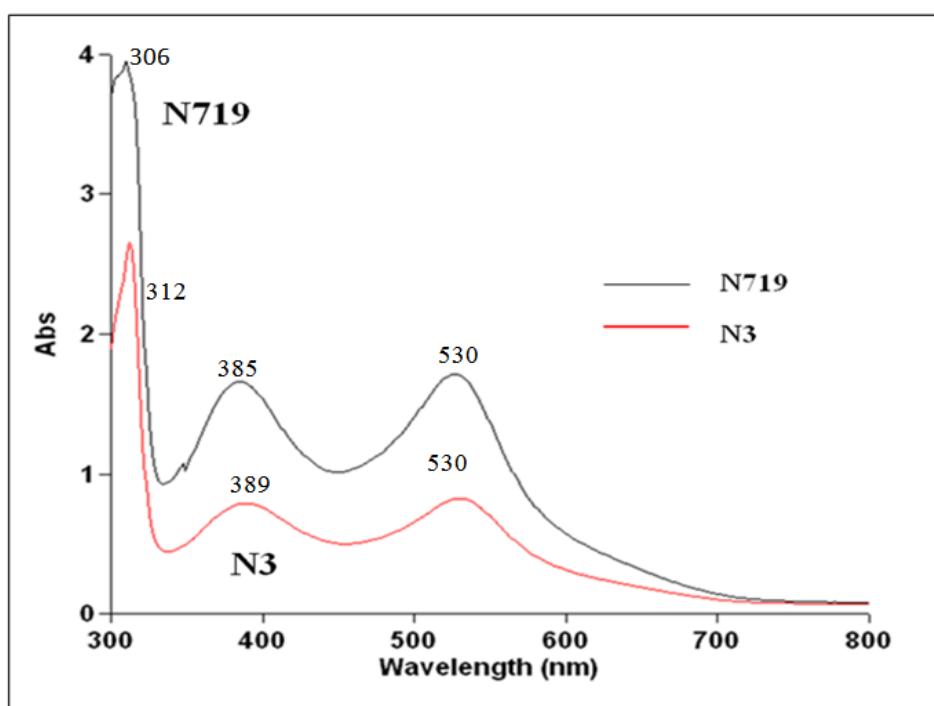


Figure 4.11: UV-visible spectroscopy for N3 and N719 dye solution

Figure 4.11 shows the variation of UV-visible absorbance of dyes solutions, (N3 and N719) of 0.3 mM. The absorption bands of N719 sensitiser are record at 530 nm and 385 nm (visible region) and 348 nm, 309 nm and 306 nm (uv region) while the absorption bands for N3 sensitiser are record 530 nm and 389 nm (visible region) and 312 nm (uv region). The absorbance bands are cause by the light adsorption of metal to ligand charge transfer transition and ligand-centered charge transfer transition, respectively.

The absorbance (N719) for the bands at 527, 385, 348, 309, 306 nm are 1.754, 1.693, 1.056, 4.015, 3.908, respectively while for N3, there are 0.825, 0.790 and 2.656, respectively. According to Lee and Huang (2009), the maximal band for N719 at visible region was at 530 nm. This is similar to that observed in this study. Similar observation is seen for N3, where the maximal band observed by Hsu, Zheng, Lin, and Ho (2005) was 534 nm, it is agreeable with the result in this study. Those bands at the visible region are directly linked to the Jsc and affected the efficiency of DSSC.

The absorption bands for these two dyes are almost identical. This is because two dyes have similar anchoring ligands, 4-4'-Dicarboxylic acid-2,2'-bipyridine (dcbpy) and ancillary ligands (NCS). Dcbpy responsible for complex adsorption onto the TiO<sub>2</sub> surface and NCS are responsible for turning the overall properties of the complexes accordance Thavasi, Renugopalakrishnan, Jose, and Ramakrishna (2009). The absorbances N719 are much higher than that of N3 due to higher uptake of photon by N719; lead to more the excitation of the dye and higher efficiency for the DSSC.

In addition, HOMO and LUMO potential energies level for N3 and N719 sensitizers. According to Stergiopoulos, Karakostas, and Falaras (2004), HOMO and LUMO of the N3 were +0.850 (V vs. SCE) and -0.750 (V vs. SCE), respectively, while the HOMO and LUMO of the N719 were +1.000 (V vs. NHE) and -0.70 (V vs. NHE), respectively (Chou, Lin, Yang, and Liu (2010)). Note that the HOMO and LUMO energies level for the N3 have to be converted to that with NHE references electrode for comparison using Equation 4.2 and the values are displays in Table 4.5.

$$E(\text{NHE}) = E(\text{SCE}) + 0.244\text{V} \quad (4.2)$$

**Table 4.5:** HOMO-LUMO energies of N3 and N719 dyes

Dyes	HOMO (V vs. NHE)	LUMO (V vs. NHE)
N3	+1.09	-0.51
N719	+1.00	-0.70

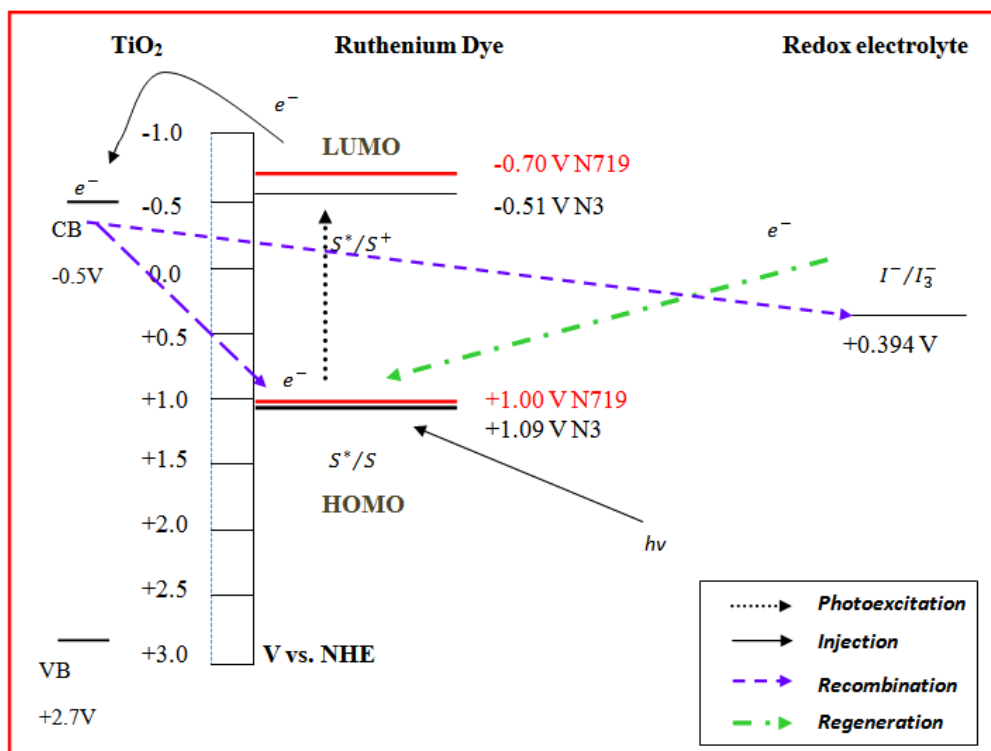


Figure 4.12: Energy level diagram for DSSC by using N3 and N719

Figure 4.12 shows that the conduction band potential of the TiO<sub>2</sub> lies at -0.5 V vs. NHE. It is clear that electron injection from the excited dye molecules into the conduction band of the semiconductor is thermodynamically possible, as the driving force for the charge displacement into the oxide is about 0.20 V for the N719 and 0.01 V for the N3. In the study of Thavasi et al. (2009), the dye/metal oxide interface needed to be designed in such a way that the oxidation potential of excited dye (LUMO) is sufficiently negative to achieve efficient electron injection into the conduction band of metal oxide. The LUMO of N719 is much more negative than the N3. Hence, N719 has higher driving force for the injection of electron to the TiO<sub>2</sub> conduction band, leads to higher  $J_{sc}$  and therefore, higher efficiency obtained.

Besides the higher driving for injected electron to the conduction band of the  $\text{TiO}_2$ , it also can explain in term of activation energy. For this view, the charge displacement into the oxide is about 0.20 V for the N719 and 0.01 V for the N3. 0.20 V is the minimum energy that able injected the electrons to the conduction band of the  $\text{TiO}_2$ . Less that this minimum energy, the electrons injected from the excited dye molecules to the  $\text{TiO}_2$  conduction band is unfavorable. Since the charge displacement into the oxide is only about 0.01 V for the N3, there are much less than this minimum energy required to start the reaction. Thus, the effective rate of the electron injected from excited N3 molecules is much lower than the N719. Thus, the efficiency of the DSSC which N719 as sensitiser is much higher than N3 and this results is disscued in section 4.1.1.

On the other hand, Figure 4.12 also show the dye regeneration is also thermodynamically favourable process, as the redox potential of  $\text{I}^-/\text{I}_3^-$  redox couple lies at +0.394 V versus NHE (above the HOMO energy level of all two complexes dyes). The higher HOMO energy level, reduction of dye cations will be easier. From the Figure 4.12, reduction of dye cations is easier for the N3 complex since N3 has higher HOMO energy level. However, the HOMO energy level for N3 and N719 is not too much different (only 0.09 V). Thus, mean that the recombination process between the injection electron and  $\text{I}^-/\text{I}_3^-$  for N3 and N719 are almost the same. This indicates in Table 4.1 where the  $V_{oc}$  for two dyes are almost the same.

## 4.2 Characterisation of DSSC with different Dye Adsorption Time

### 4.2.1 I-V Test

**Table 4.6:** Photovoltaic performance of DSSC with N3 sensitiser at different dye adsorption time

<b>Dye adsorption time (Hour)</b>	<b>Efficiency, <math>\eta</math> (%)</b>	<b>Fill factor, FF</b>	<b>Open circuit voltage, Voc (V)</b>	<b>Current density, Jsc (mA/cm<sup>2</sup>)</b>
10	3.38	0.62	0.65	8.41
12	3.68	0.65	0.64	8.79
14	4.34	0.66	0.68	9.67
16	4.77	0.70	0.64	10.56
18	4.84	0.66	0.67	10.91
20	5.73	0.66	0.62	14.27
22	6.04	0.69	0.63	14.00
24	6.61	0.70	0.64	14.77
26	6.23	0.70	0.61	14.67
28	5.86	0.67	0.63	13.88
30	5.64	0.65	0.62	14.01

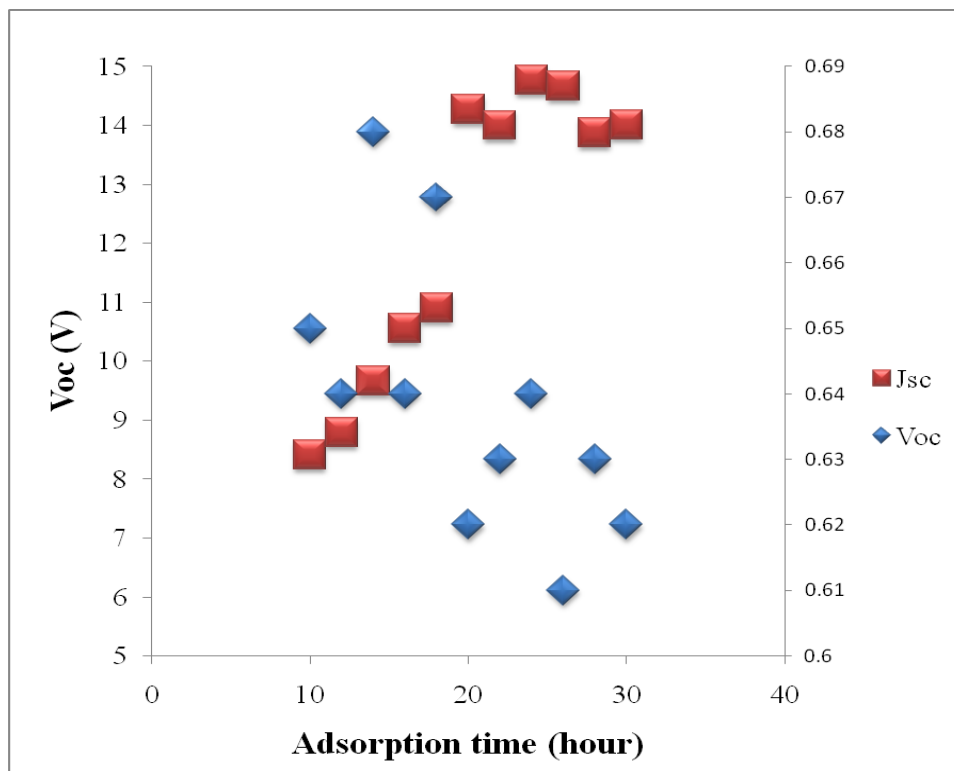


Figure 4.13: Variation of  $V_{oc}$  and  $J_{sc}$  with time for N3-DSSC

Table 4.6 is photovoltaic performances of N3 with different dye adsorption time. Figure 4.13 is sketched based on the data of the Table 4.6 to show the variation of  $V_{oc}$  and  $J_{sc}$  with time for the N3-DSSC. No trend is observed in the  $V_{oc}$  while the  $J_{sc}$  is increase linearly with the adsorption time up to 24 hours followed by an almost constant value. This proven that the sample is saturated with dye molecules after 24 hours accordance to Kim et al. (2010). Therefore, the DSSC should achieve a maximum efficiency at 24 hours (Figure 4.14).

From Table 4.6, there are not much variation is observed in the  $V_{oc}$  and FF, within the range of 0.6 to 0.7. On the other hand, a big increase is seen in  $J_{sc}$  from 8.41 mA/cm<sup>2</sup> (10 hours) to 14.77 mA/cm<sup>2</sup> (24 hours), more electrons are photo-excited and emitted, thus output current and efficiency of DSSC increase with increase the adsorption time. Similar result is obtained in the study of Kim et al. (2010).



According to Kim et al. (2010), the  $J_{sc}$  is a dominant factor affecting the efficiency can be expressed by the following equation:

$$J_{sc} = \int q F(\lambda) [1 - r(\lambda)] LHE(\lambda) \Phi_{ET}(\lambda) d\lambda \quad (4.3)$$

Where  $q$  is the electron charge,  $F(\lambda)$  is the incident light loss due to light adsorption and reflection by the conducting glass, LHE is light harvesting efficiency and  $\Phi_{ET}(\lambda)$  is defined as the electron transfer yield. According to Equation 4.3,  $J_{sc}$  increases in proportion to LHE ( $\lambda$ ). The more light harvesting efficiency, the more  $J_{sc}$  increases and hence higher efficiency of the DSSC.

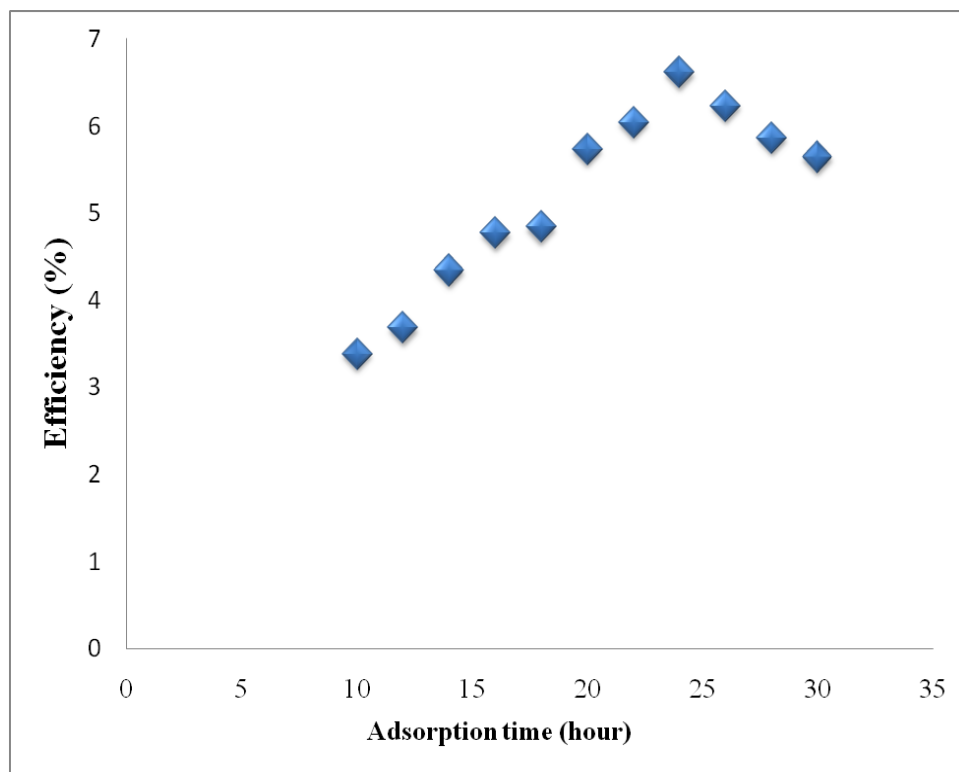


Figure 4.14: Variation of efficiency with time for N3-DSSC.

**Table 4.7:** Photovoltaic performance of DSSC with N719 sensitiser at different dye adsorption time

<b>Dye adsorption time (Hour)</b>	<b>Efficiency, <math>\eta</math> (%)</b>	<b>Fill factor, FF</b>	<b>Open circuit voltage, Voc (V)</b>	<b>Current density, Jsc (mA/cm<sup>2</sup>)</b>
10	5.59	0.68	0.68	11.98
12	5.65	0.70	0.63	12.57
14	5.97	0.63	0.69	13.84
16	7.30	0.70	0.62	16.63
18	7.51	0.70	0.62	17.18
20	7.55	0.70	0.63	17.17
22	8.29	0.71	0.67	17.39
24	8.53	0.70	0.71	17.23
26	7.89	0.64	0.66	18.52
28	7.60	0.68	0.61	18.19
30	7.27	0.67	0.62	17.47

Similar dye soaking experiment carried out for the N719 sensitiser. Table 4.7 is the summary of comparison between the photovoltaic performances of N719 with different dye adsorption time. Figure 4.15 and 4.16 are sketched based on the data of the Table 4.6 to show the variation of  $V_{oc}$ ,  $J_{sc}$ , and efficiency with time for the N719-DSSC. This experiment is shows the same observation with the N3-DSSC. (Results obtained from this section refer appendix G and H)

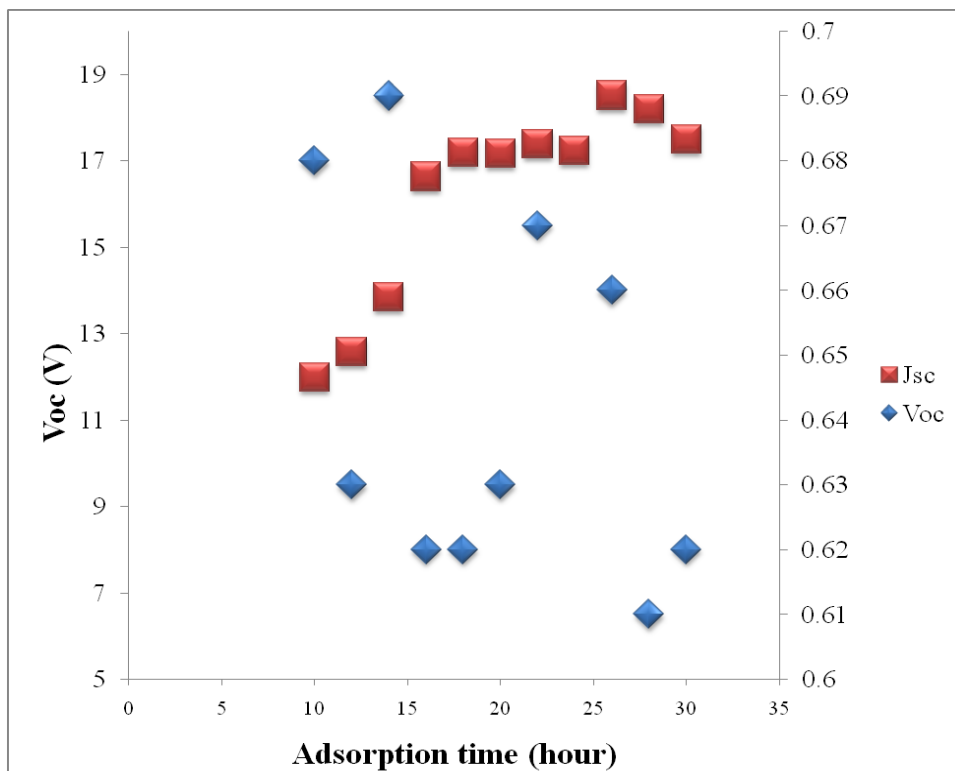


Figure 4.15: Variation of  $V_{oc}$  and  $J_{sc}$  with time for N719-DSSC

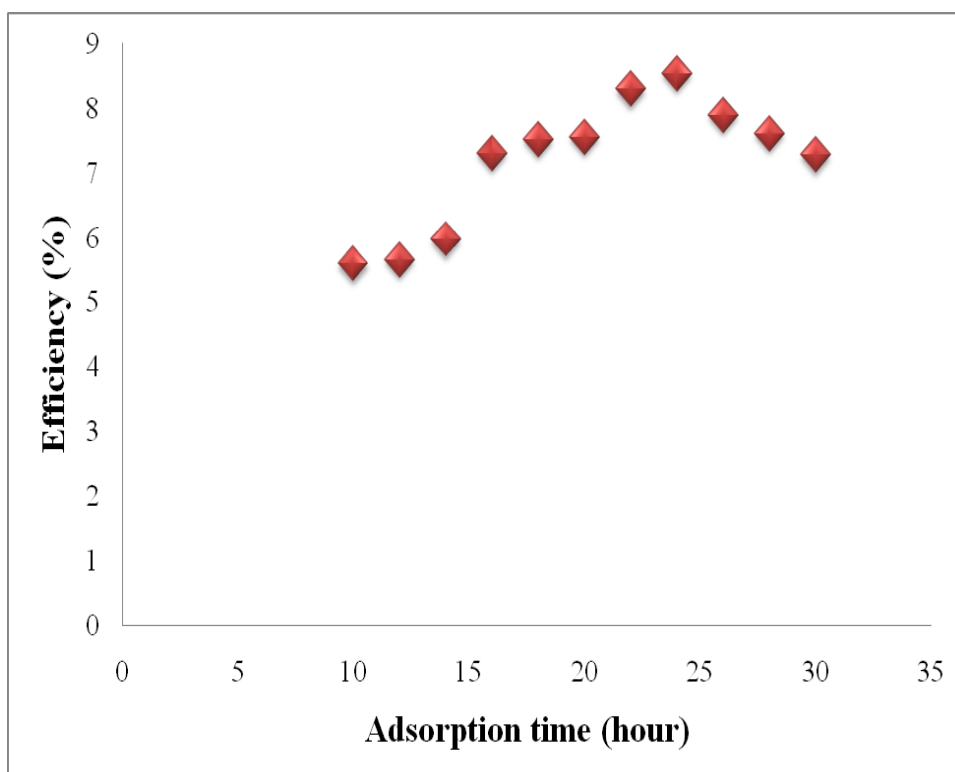


Figure 4.16: Variation of efficiency with time for N719-DSSC

### 4.2.2 Dye Loading

A mixed solvent of absolute ethanol and 0.1 M NaOH (volume ratio=1:1) solution is used in the UV-vis spectroscopic study. According to Katoh, Yaguchi, Murai, Watanabe, and Furube (2010), concentration of the solution which used for dye adsorption measurement should be less than 0.05 mM. This is because small precipitate is observed at solution concentration above 0.1 mM. Thus, 0.04 mM of the solvent is used in this study according the above explanation.

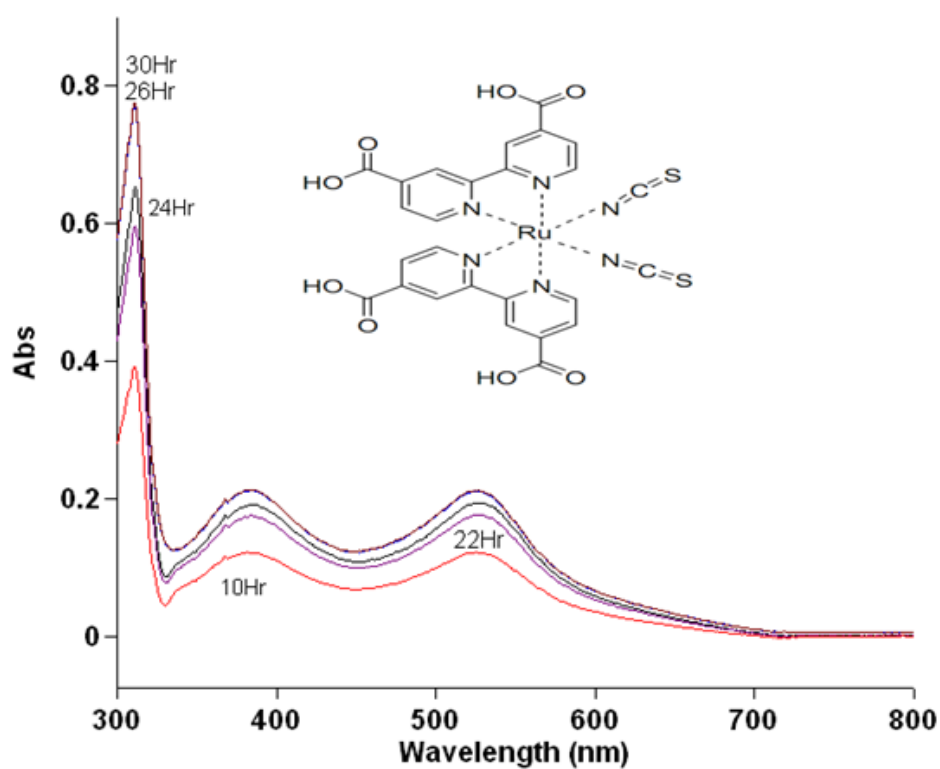


Figure 4.17: Absorption spectra of TiO<sub>2</sub>/N3

**Table 4.8:** Adsorption bands and absorbance of TiO<sub>2</sub>/N3 at different immersion time

<b>Dye adsorption time (Hour)</b>	<b>Adsorption Peaks (nm)</b>	<b>Absorbance</b>
<b>10 Hour</b>	525	0.122
	382	0.122
	311	0.390
<b>22 Hour</b>	525	0.176
	384	0.175
	311	0.595
<b>24 Hour</b>	530	0.194
	385	0.191
	311	0.653
<b>26 Hour</b>	524	0.211
	384	0.212
	311	0.773
<b>30 Hour</b>	524	0.212
	384	0.213
	311	0.776

Figure 4.17 shows the absorption spectra of N3 dye adsorbed on TiO<sub>2</sub> nanocrystalline film (TiO<sub>2</sub>/N3) with different immersion hours. From the figure, it is seen that the absorbance increases with the increase of immersion time due to the increase of the amount of dye molecules adsorbed on the TiO<sub>2</sub>. However, the optimal dye adsorption happens at the immersion time of 24 hours, indicating the full coverage of the dye molecules on the TiO<sub>2</sub> surface. Further increase in the immersion time would result in the formation of a multi-dye adsorption layer on the TiO<sub>2</sub> film (increase absorbance), promoting the aggregation that would cause a decrease in electron injection efficiency. This is proven by the decrease in the adsorption band as observed in Table 4.8. According to Katoh et al. (2010), the multi-layer adsorption of the dyes on the TiO<sub>2</sub> film surface would decrease the electron injection efficiency. Thus, lower efficiency is obtained for higher immersion time.

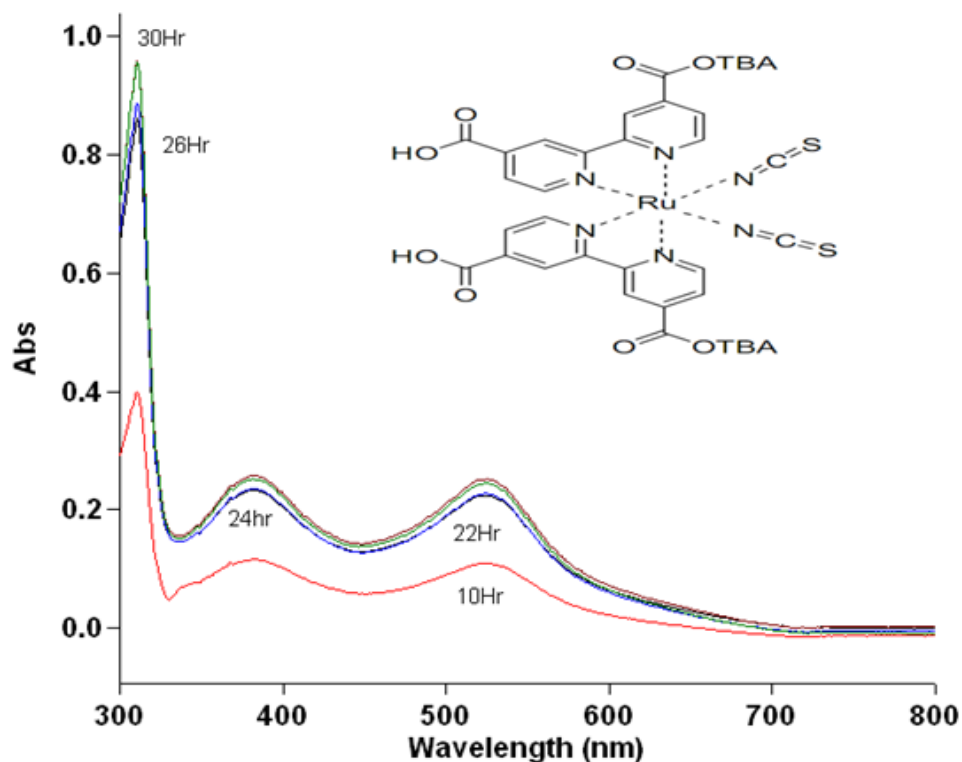


Figure 4.18: Absorption spectra of N719/TiO<sub>2</sub> at different immersion time

Figure 4.18 show the absorption spectra of N719/TiO<sub>2</sub> with different immersion times. The absorption bands for different dye adsorption periods is summarised in Table 4.9. From Figure 4.18, found that the absorbance versus wavelength curves for different immersion times is similar with the TiO<sub>2</sub>/N3 condition. Thus, explanation for this is similar for the TiO<sub>2</sub>/N3 condition which discussed above. Nevertheless, found the aggregation is expected to be reduced for N719/TiO<sub>2</sub> as compared between the TiO<sub>2</sub>/N3 and N719/TiO<sub>2</sub> films. This is because the TBA<sup>+</sup> groups that substituted the H<sup>+</sup> groups for the molecular structure of the N719 which discuss in 4.1.1 section. Hence, the N719 sensitizer DSSC has given higher efficiency than N3 sensitizer in this work. Table 4.9 is summarised the adsorption bands and absorbance of N719 dye adsorbed on TiO<sub>2</sub> nanocrystalline film which fabricated under difference immersion times.

**Table 4.9:** Adsorption bands and absorbance of N719/TiO<sub>2</sub> at different immersion time

<b>Dye adsorption time (Hour)</b>	<b>Adsorption Peaks (nm)</b>	<b>Absorbance</b>
<b>10 Hour</b>	525	0.110
	381	0.110
	310	0.398
<b>22 Hour</b>	530	0.224
	382	0.233
	310	0.861
<b>24 Hour</b>	534	0.227
	385	0.235
	310	0.887
<b>26 Hour</b>	525	0.245
	385	0.252
	310	0.956
<b>30 Hour</b>	525	0.252
	384	0.257
	310	0.959

## CHAPTER 5

### CONCLUSION AND RECOMMENDATIONS

#### 5.1 Conclusion

This project includes 2 parts: Characterisation of different sensitiser, and effect of dye loading on the efficiency of the DSSC. Besides, problems encountered and recommendations are provided for further improvement of the research.

##### 5.1.1 Characterisation of DSSC for different Sensitisers

Comparison between N3 and N719 performance by using I-V test, dye loading measurement, X-ray diffraction, SEM images, it shows that the N719 sensitiser performed better than N3 sensitiser.

N719 give better photovoltaic performance than N3 because of the substitution of the TBA group in the N719 molecular structure. The consequences is higher driving force provides and lesser dye aggregated problem than N3. Hence, the  $J_{sc}$  and efficiency of N719 is higher than N3. Besides, N719 given higher absorbance than N3 since the more electrons injected from the excited dye to the conduction band of the  $TiO_2$ .



### 5.1.2 Effect of Dye Loading

The dye soaking times study shows the relationship between the dyes adsorption times periods and the cell performance. It is conclude that the 24 dye adsorption hours is the optimal adsorption period because it given the best photovoltaic performance of both  $\text{TiO}_2/\text{N3}$  and  $\text{TiO}_2/\text{N719}$ . Continuous immersion over 24 hours, the dye likely aggregated and result slower electron injection from excited dye to the  $\text{TiO}_2$  conduction band. Hence, lower efficiency of the DSSC.

## 5.2 Problems Encountered and Solutions

During the fabrication of the DSSC, two major problems have been encountered. First problem is on the cell assembly where there is a need to seal the photoanode with the counter electrode. The recommended temperature for the type of sealant used in this project is 110 to 130°C. However, this temperature range discovered that is unable to seal the two electrodes effectively. Then, electrolyte leakages are the consequence of poor cell assembly. Figure 5.1 indicates the electrolyte leakages from poor cell assembly.

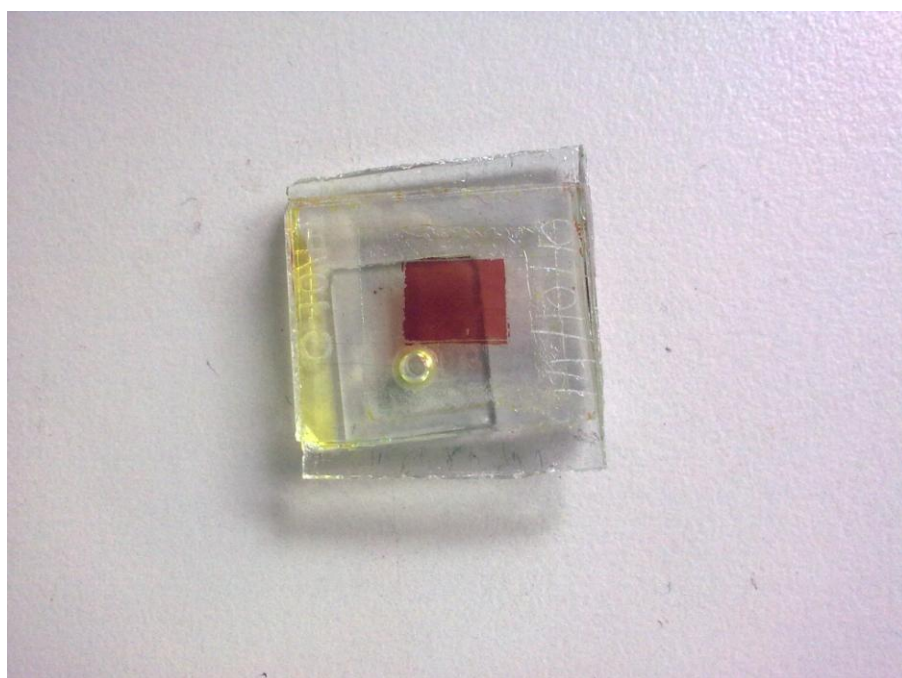


Figure 5.1: Electrolyte leakages from poor cell assembly

From the experiments, this poor cell assembly problem can be overcome by increasing sealing temperature to 150°C and then slowly cool to room temperature. This method not only improves the sealing of the two electrodes effectively, it also prevents cracks formation on the TiO<sub>2</sub>/dye surface.

Second problem is encountered during injection of electrolyte into the cell. Electrolyte can easily evaporate even DSSC is seal effectively. This main reason is that excess electrolytes still surround the hole in the counter electrode. Therefore, electrolytes easily evaporate and it affects the stability of the DSSC. Solution to overcome this problem is using edge of tissue to remove the excess electrolytes surrounding the hole in the counter electrode. Therefore, the stability of the DSSC can be increased and efficiency obtained is relatively consistent even after 1 week fabrication. This method is shown in Figure 5.2 where excess electrolytes are removed from the through hole by tissue.



Figure 5.2: Remove excess electrolytes by tissue.

### 5.3 Recommendations

More studies such as Impedance spectroscopy need to do on validating the relationship between dye adsorption to the  $\text{TiO}_2$  surface and the resistance about electron transfer at  $\text{TiO}_2$ /dye/electrolyte interfaces. Besides, transient adsorption (TA) techniques need to use for evaluated the recombination rate between the dye cation and electron in photoanode. These two further studies could able to justify this work result.

Besides, other types of dye (with different functional group) such as natural dye and dye adsorption condition (example, dye concentration etc.) should carry out for investigated the effect of different dye to the DSSC performance. This is because the N3 and N719 dyes that used in this work are belong to the same functional group and ligands. Thus, the effect is not too much significant toward the DSSC performance.

Furthermore, other fabrication techniques such as screen printing and sol-gel are recommended to carry out which used to apply the  $\text{TiO}_2$  paste onto the FTO glass surface. This is because it would more likely to produce an even  $\text{TiO}_2$  film surfaces. Besides, these techniques also reduce the possibility of crack formation on the  $\text{TiO}_2$  films surface which tend to bad result on electron transport path. Therefore, high efficiency of the DSSC is able to obtain.

In addition, much more dye adsorption periods should carry out on validating the relationship between the adsorption times and the DSSC efficiency. The dye adsorption periods should set from 0 to 30 hour. This recommendation is suggested because there are not enough raw materials or resources for this work in order develop 0 to 30 dye adsorption periods.

Lastly, the experiments should carry out under the control environment in order to avoid the contaminants during the DSSC fabrication. This is because many researchers found that the DSSC efficiency is dramatically decreased with the effect of contaminates.

## REFERENCES

- Chou, C.S., Lin, Y.J., Yang, R.Y., & Liu, K.H. (2011). Preparation of TiO<sub>2</sub>/ NiO composite particles and their applications in dye sensitized solar cells. *Advance Powder Technology*, 22(1), 31-42.
- Lenzmann, F. O., & Kroon, J.M. (2007). Recent advances in Dye-Sensitized Solar Cells. *Advances in Optoelectronics*, 2007, 1-10.
- Kantonis, G., Stergiopoulos, T., Katsoulidis, A. P., Pomonis, P. J., & Falaras, P. (2011). Electron dynamics dependence on optimum dye loading for an efficient dye-sensitized solar cell. *Journal of photochemistry and photobiology A: Chemistry*, 217, 236-241.
- Vougioukalakis, G. C., Philippopoulos, A. I., Stergiopoulos, T., & Falaras, P. (2010). Contributions to the development of ruthenium-based sensitizers for dye-sensitized solar cells. *Coordination Chemistry Reviews*.
- Boschloo, G., Edvinsson, T., & Hagfeldt, A. (2006). Dye sensitized nanostructured ZnO electrodes for solar cell application. *Nanostructure Materials for Solar Energy Conversion* (p. 227-243). United Kingdom: Elsevier B.V.
- Gratzel, M. (2003). Review dye-sensitized solar cells. *Journal of Photochemistry and Photobiology C: Photochemistry Reviews*, 4, 145-153.
- Kisserwan, H., & Ghaddar, T.H. (2010). Enhancement of photovoltaic performance of a novel dye, 'T18', with ketene thioacetal groups as electron donors for high efficiency dye-sensitized solar cell. *Inorganic Chimica Acta*, 363, 2409-2415.

Uam, H. S., Jung, Y. S., Jun, Y. S., & Kim, K. J. (2010). Relation of Ru (II) dye desorption from TiO<sub>2</sub> film during illumination with photocurrent decrease of dye-sensitized solar cells. *Journal of photochemistry and photobiology A: Chemistry*, 212, 122-128.

Chang, H., Su, H. T., Chen, W. A., Huang, K. D., Chien, S. H., Chen, S. L., et al. (2009). Fabrication of multiple TiO<sub>2</sub> thin film for dye sensitized solar cell with high conversion efficiency by electrophoresis deposition. *Solar Energy*, 84, 130-136.

Koo, H. J., Park, J., Yoo, B., Yoo, K., Kim, K. K., & Park, N. G. (2007). Size dependent scattering efficiency in dye sensitized solar cell. *Inorganic Chimica Acta*, 361, 677-683.

Seo, H. W., Son, M. K., Kim, J. K., Lee, K. J., Prabakar, K., & Kim, H. J. (2010). Faster dye-adsorption of dye-sensitized solar cells by applying an electric field. *Electrochimica Acta*, 55, 4120-4123.

Kim, J. K., Seo, H. W., Son, M. K., Shin, I., Hong, J. T., & Kim, H. J. (2010). The analysis of the change in the performance and impedance of dye-sensitized solar cell according to dye-adsorption time. *Current Applied Physics*, 10 (3), S418-S421.

Lee, K. M., Hsu, Y. C., Ikegami, M., Miyasaka, T., Thomas K. J., Lin, J. T., et al. (2011). Co-sensitization promoted light harvesting for plastic dye sensitized solar cells. *Journal of Power Sources*, 196, 2416-2421.

Hwang, K. J., Jung, S. H., Park, D. W., Yoo, S. J., & Lee, J. W. (2010). Heterogeneous ruthenium dye adsorption on non-structured TiO<sub>2</sub> films for dye-sensitized solar cells. *Current Applied Physics*, 10, 5184-5187.

Yang, L., Lin, Y., Jia, J., Xiao, X., Li, X., & Zhu, X. W. (2008). Light harvesting enhancement for dye-sensitized solar cell by novel anode containing cauliflower-like TiO<sub>2</sub> spheres. *Journal of Power Source*, 182, 370-376.

Lee, R. H., & Huang, Y. W. (2009). Enhancing the photovoltaic performance of dye-sensitized solar-cells by modifying the TiO<sub>2</sub> electrode-sensitized dye interface. *Thin Solid Films*, 517, 5903-5908.

Yaguchi, K., Katoh, R., Murai, M., Watanabe, S., & Furube, A. (2010). Differences in adsorption behaviour of N3 dye on flat and nanoporous TiO<sub>2</sub> surfaces. *Chemical Physics Letters*, 497, 48-51.

Katoh, R., Kasuya, M., Furube, A., Fuke, N., Koide, N., & Han, L. (2009). Recombination rate between dye cations and electrons in N719-sensitized nanocrystalline TiO<sub>2</sub> films under substantially weak excitation conditions. *Chemical Physics Letters*, 489, 280-282.

Katoh, R., Fuke, N., Furube, A., & Koide, N. (2010). Effect of the dye coverage on photo-induced electron injection efficiency in N719-sensitized nanocrystalline TiO<sub>2</sub> films. *Chemical Physics Letters*, 471, 202-206.

Hore, S., Vetter, C., Kern, R., Smit, N., & Hirsch, A. (2005). Influence of scattering layers on efficiency of dye-sensitized solar cells. *Solar Energy Materials and Solar Cell*, 1176-1188.

Satyen, K. D. (2005). Dye sensitized TiO<sub>2</sub> thin film solar cell research at the National Renewable Energy Laboratory (NREL). *Solar Energy Materials & Solar Cells*, 1-10.

Ito, S., Murakami, T. N., Comte, P., Liska, P., Gratzel, C., Nazeerudin, M. K., et al. (2008). Fabrication of thin film dye sensitized solar cell with solar to electric power conversion efficiency over 10%. *Thin Solid Film*, 516, 4613-4619.

Mori, S., & Yanagida, S. (2006). TiO<sub>2</sub> based dye sensitized solar cell. *Nanostructure Materials for Solar Energy Conversion* (pp. 193-225). United Kingdom: Elsevier B.V.

Jang, S. R., Choi, M. J., Vital, R., & Kim, K. J. (2007). Anchorage of N3 dye-linked polyacrylic acid to TiO<sub>2</sub>/electrolyte interface for improvement in the performance of Dye-sensitized solar cell. *Solar Energy Materials & Solar Cells*, 1209-1214.

Ngamsinlapasathin, S., Srcehawong, T., Suzuki, Y., & Yoshikawa, S. (2005). Single and double layered mesoporous TiO<sub>2</sub>/ P25 TiO<sub>2</sub> electrode for dye sensitized solar cell. *Solar Energy Materials and Solar Cell*, 86 (2), 269-282.

Dhungel, S. K., & Park, J. G. (2010). Optimization of apste formulation for TiO<sub>2</sub> nonoparticles with wide range of site distribution for its application in dye sensitized solar cell. *Renewable Energy* , 1-5.

Hwang, S. Y., Lee, J. H., Park, C. M., Lee, H. L., Kim, C. Y., Park, C. Y., et al. (2007). A highly efficient organic sensitizer for dye-sensitized solar cell. *Chemistry Communication* , 4887-4888.

Stergiopoulos, T., Karakostas, S., & Falaras, P. (2004). Comparative studies of substituted rethenium (II)-pyrazoyl-pyridine complexes with classical N3 phoyosensitizer: the influence of NCS dye ligands on the efficiency of solid state nanocrystalline solar cells. *Journal of Photochemistry and Photobiology A: Chemistry* , 163, 331-340.

Yamaguchi, T., Uchida, Y., Agatsuma, S., & Arakawa, H. (2009). Series connected tandem dye-sensitized solar cell for improving efficiency of more than 10%. *Solar Energy Material and Solar Cell* , 93, 733-736.

Thavasi, V., Renugopalakrishnan, V., Jose, R., & Ramakrishna, S. (2009). Controlled electron injection and trasport at materials interfaces in dye sensitized solar cells. *Materials Science and Engineering R63* , 81-99.

Wu, W., Guo, F., Li, J., He, J. X., & Hua, J. L. (2010). New Fluoranthene based cyanine dye for dye sensitized solar cell. *Synthetic Metals* , 160, 1008-1014.

Chiba, Y., Islam, A., Watanabe, Y., Komiya, R., Koide, N., & Han, L. (2006). Dye sensitized solar cell with conversion efficiency of 11.9%. *Japanese Journal of Applied Physics part2* , 45 (25), L638-L640.

Ogomi, Y., Kaashiwa, Y., Naoma, Y., Fujita, Y., Kojima, S., Kono, M., et al. (2009). Photovoltaic performance of sye-sensitized solar cell stained with balck dye under preseeurized condition and mechanism for high efficiency. *Solar Material and Solar Cell* , 1009-1012.

Dittrich, T., Ofir, A., Tirosh, S., Grinis, L., Zaban, A. (2006). Influence of the porosity on diffusion and lifetime in porous TiO<sub>2</sub> layers. *Applied Physics Letters*, 88, 182110-1 – 182110-2



Kawakita, J. (2010). Trends of research and development of Dye-Sensitized solar cells. *Science & Technology Trends*, 35, 70-82.

Wang, Z. S., Kawauchi, H., Kashima, T., & Arakawa, H. (2004). Significant influence of TiO<sub>2</sub> photoelectrode morphology on the energy conversion efficiency of N719 dye-sensitized solar cell. *Coordination Chemistry Reviews*, 1381-1389.

Lee, W. P. (2010). Kinetic and Thermal Study of Dye Adsorption on TiO<sub>2</sub> and Sequential Dye Adsorption Model for Dye sensitized Solar Cells (DSSC). Degree Thesis, Nanyang Technological University, Singapore.

Marinado, T. (2009) Photoelectrochemical studies of dye-sensitized solar cells using organic dyes. *Electronic references*.

Retrieved October 3, 2010,

from

[http://www.google.com.my/#hl=en&source=hp&biw=1280&bih=616&q=Tannia.+Marinado.+&btnG=Google+Search&oq=Tannia.+Marinado.+&aq=f&aqi=&aql=&gs\\_sm=s&gs\\_upl=5187841518784101111010101010101&fp=d7045a660e0e35dd](http://www.google.com.my/#hl=en&source=hp&biw=1280&bih=616&q=Tannia.+Marinado.+&btnG=Google+Search&oq=Tannia.+Marinado.+&aq=f&aqi=&aql=&gs_sm=s&gs_upl=5187841518784101111010101010101&fp=d7045a660e0e35dd)

Char, K. H. (2010). Chapter 5: Dye Sensitized Solar Cells (DSSC). *Electronic references*.

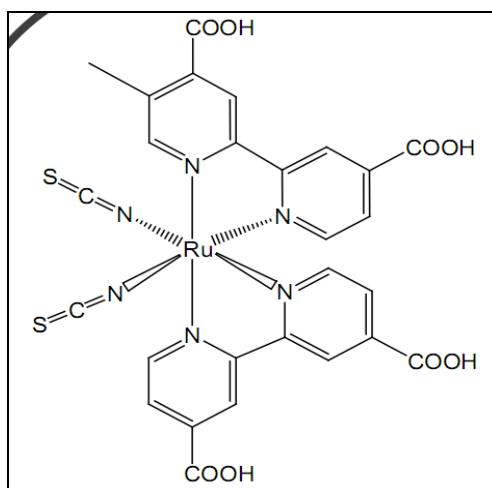
Retrieved March 31, 2011,

from

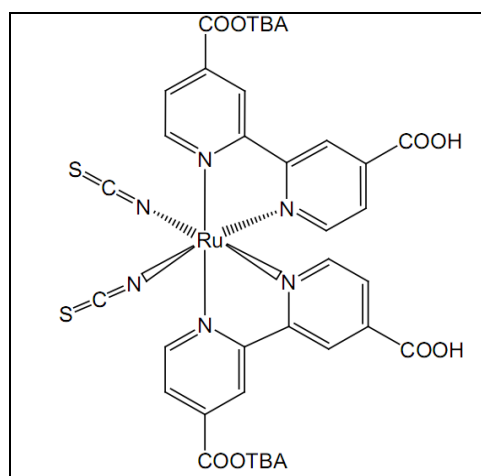
[http://www.kocw.net/home/common/contents/document/wcu/2010/11/06/05/11\\_06\\_05\\_05.pdf](http://www.kocw.net/home/common/contents/document/wcu/2010/11/06/05/11_06_05_05.pdf)

**APPENDICES**

## APPENDIX A: Molecules structure of N3 and N719 (Char, 2010)

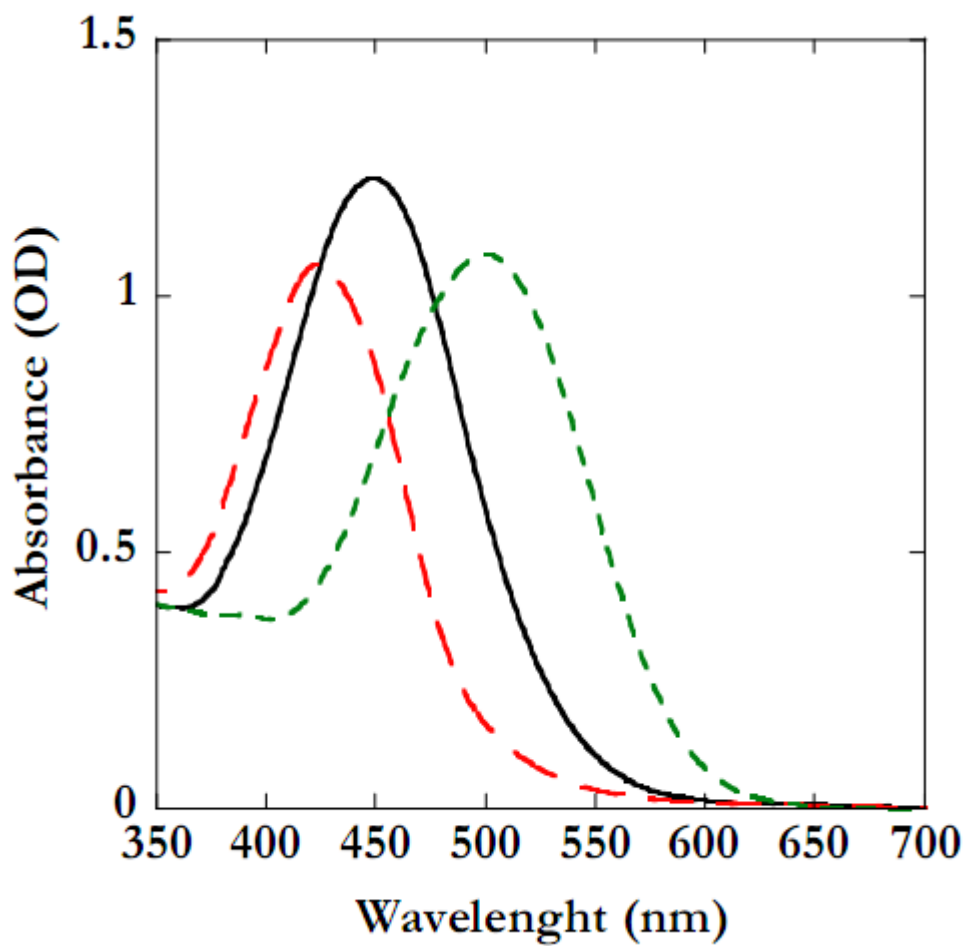


N3



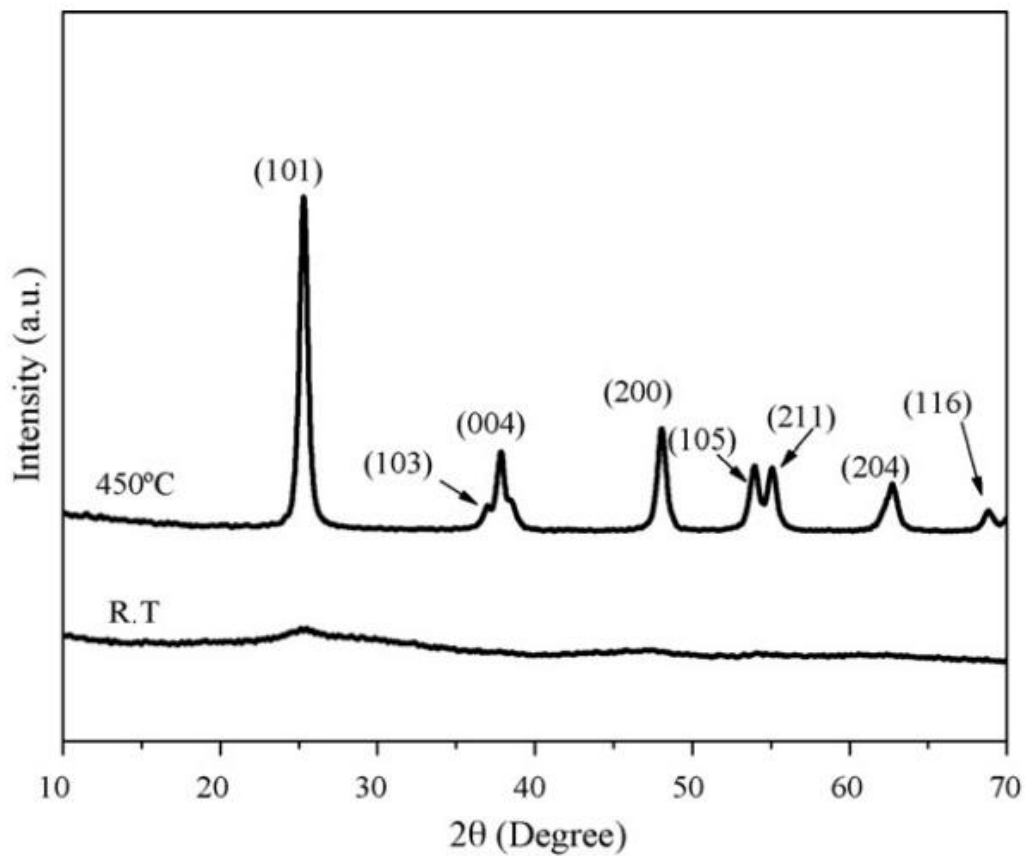
N719

## APPENDIX B: Solvent Effect (Marinado, 2009)



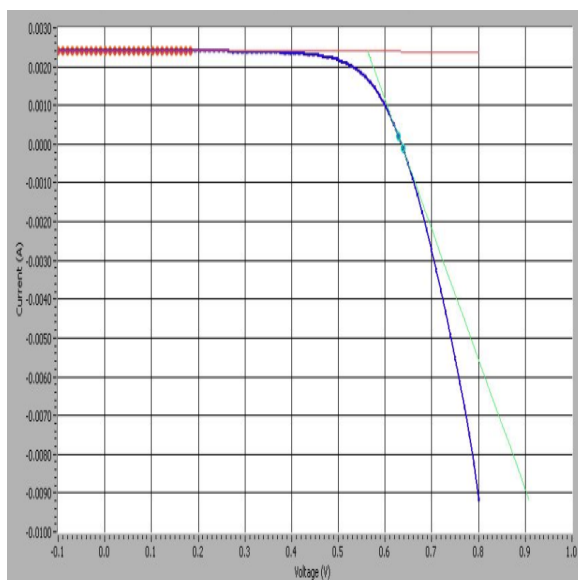
Appendix B shows absorption spectra of ethanol ( — ) and acetonitrile ( - - - )

## APPENDIX C: X-ray pattern (Yang et al., 2009)



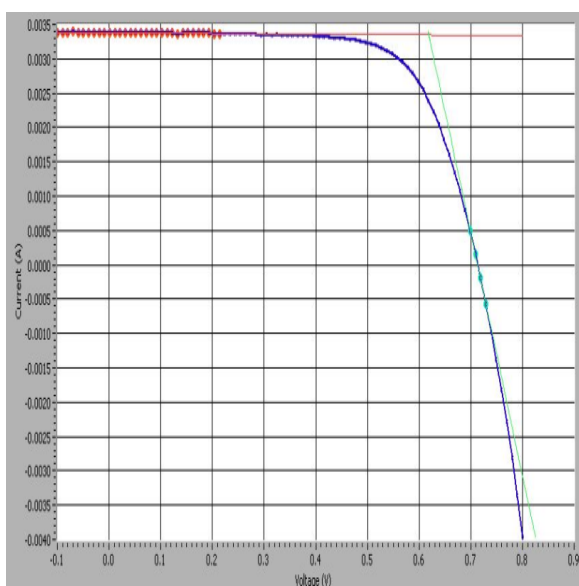
X-ray pattern for the TiO<sub>2</sub> paste which undergoes 450°C sintered.

## APPENDIX D: I-V Test result for N3 and N719 sensitizers



Voc (V)	0.6346
Isc (A)	0.0024
Jsc (mA/cm <sup>2</sup> )	14.5146
Imax (A)	0.0021
Vmax (V)	0.5050
Pmax (mW)	1.0856
Fill Factor (%)	71.4252
Efficiency (%)	6.5794
R at Voc	29.8457
R at Isc	97264.1293

Photovoltaic measurement for DSSC which used N3 as sensitizer



Voc (V)	0.7132
Isc (A)	0.0034
Jsc (mA/cm <sup>2</sup> )	16.8936
Imax (A)	0.0030
Vmax (V)	0.5530
Pmax (mW)	1.6864
Fill Factor (%)	69.9867
Efficiency (%)	8.4321
R at Voc	28.1685
R at Isc	20692.1243

Photovoltaic measurement for DSSC which used N719 as sensitizer

## APPENDIX E: UV visible spectrophotometer result for N3 and N719 dye solution

## Scan Analysis Report

Report Time : Wed 09 Mar 04:32:53 PM 2011

Method:

Batch: C:\Documents and Settings\fes\Desktop\Dr. Liang\yian\dye solution.DSW

Software version: 3.00(339)

Operator:

### Sample Name: N3

Collection Time 3/9/2011 4:35:12 PM

Peak Table

Peak Style

Peaks

Peak Threshold

0.0100

Range

800.00nm to 300.00nm

Wavelength (nm)	Abs
530.00	0.825
389.00	0.790
312.00	2.656

## Scan Analysis Report

Report Time : Wed 09 Mar 04:17:24 PM 2011

Method:

Batch: C:\Documents and Settings\fes\Desktop\Dr. Liang\yian\dye solution1.DSW

Software version: 3.00(339)

Operator:

### Sample Name: N719

Collection Time 3/9/2011 4:17:29 PM

Peak Table

Peak Style

Peaks

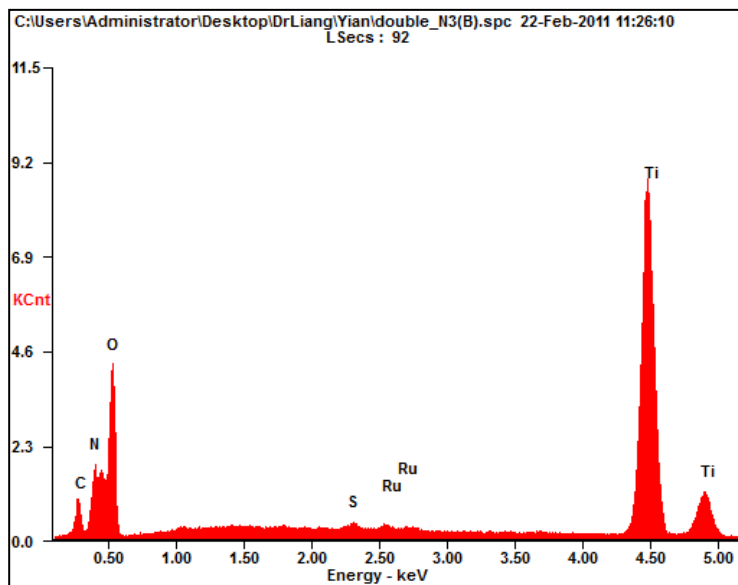
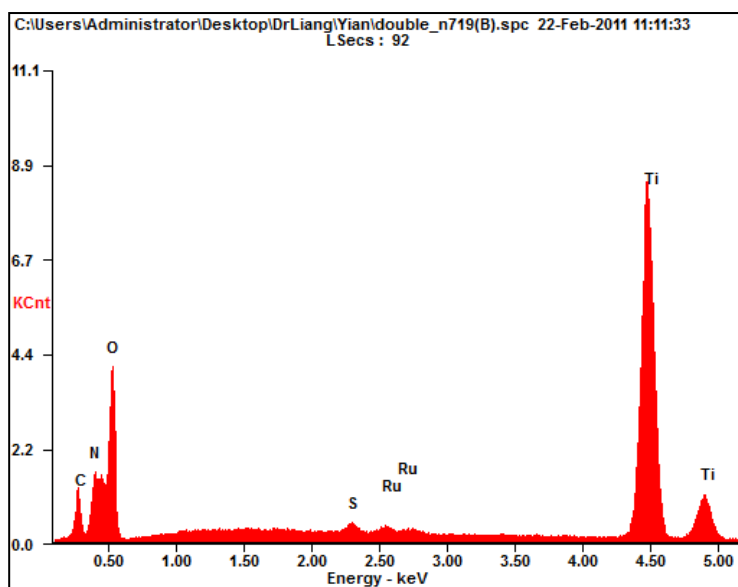
Peak Threshold

0.0100

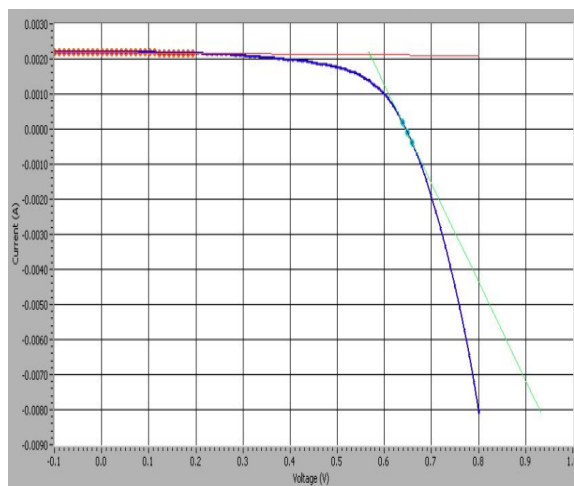
Range

800.00nm to 300.00nm

Wavelength (nm)	Abs
530.00	1.754
385.00	1.693
348.00	1.056
309.00	4.015
306.00	3.908

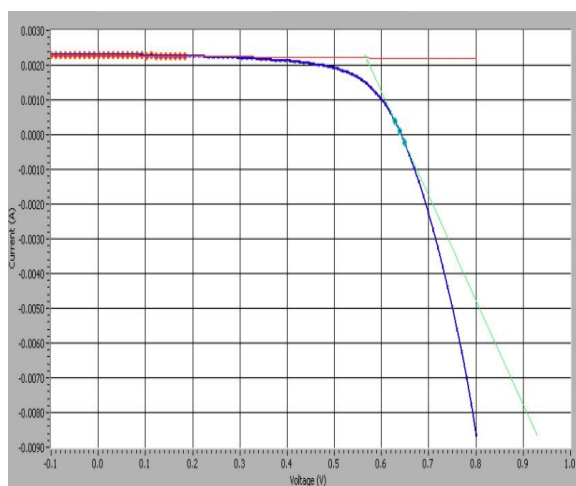
APPENDIX F: EDS results for TiO<sub>2</sub>/N3 film and TiO<sub>2</sub>/ N719 filmEDS results for N3/TiO<sub>2</sub> filmEDS results for N719/TiO<sub>2</sub> film

## APPENDIX G: I-V Test results for DSSC with N3



Voc (V)	0.6450
Isc (A)	0.0022
Jsc (mA/cm <sup>2</sup> )	8.4064
Imax (A)	0.0017
Vmax (V)	0.5033
Pmax (mW)	0.8799
Fill Factor (%)	62.4100
Efficiency (%)	3.3841
R at Voc	35.5512
R at Isc	9012.2952

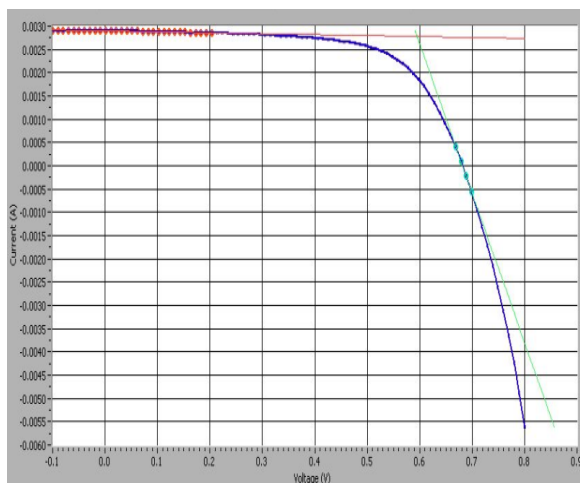
DSSC which used N3 sensitizer (10 immersion hours)



Voc (V)	0.6411
Isc (A)	0.0023
Jsc (mA/cm <sup>2</sup> )	8.7945
Imax (A)	0.0019
Vmax (V)	0.5041
Pmax (mW)	0.9573
Fill Factor (%)	65.3069
Efficiency (%)	3.6819
R at Voc	33.3227
R at Isc	7422.0567

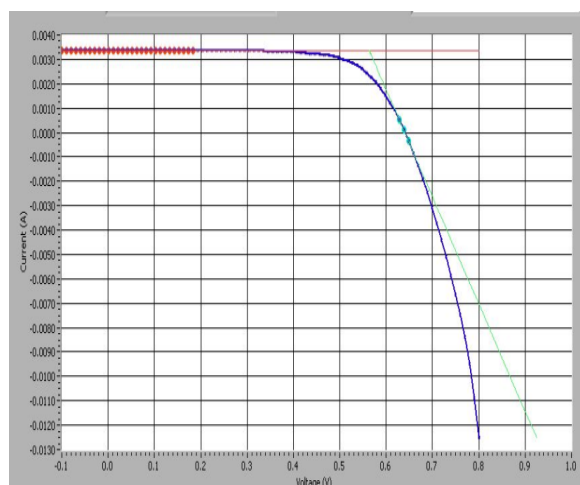
DSSC which used N3 sensitizer (12 immersion hours)





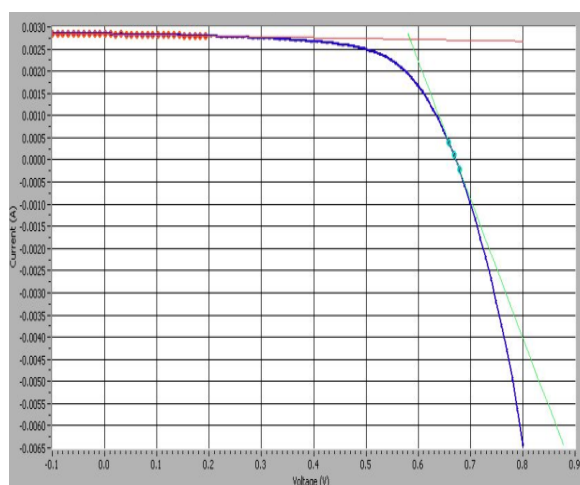
Voc (V)	0.6816
Isc (A)	0.0029
Jsc (mA/cm <sup>2</sup> )	9.6657
Imax (A)	0.0025
Vmax (V)	0.5250
Pmax (mW)	1.3005
Fill Factor (%)	65.7975
Efficiency (%)	4.3351
R at Voc	31.1616
R at Isc	5001.5006

DSSC which used N3 sensitizer (14 immersion hours)



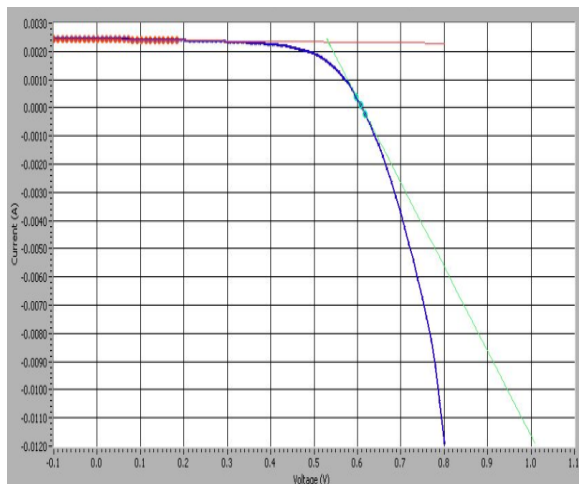
Voc (V)	0.6402
Isc (A)	0.0034
Jsc (mA/cm <sup>2</sup> )	10.5581
Imax (A)	0.0030
Vmax (V)	0.5040
Pmax (mW)	1.5269
Fill Factor (%)	70.5949
Efficiency (%)	4.7716
R at Voc	22.7047
R at Isc	174605.7004

DSSC which used N3 sensitizer (16 immersion hours)



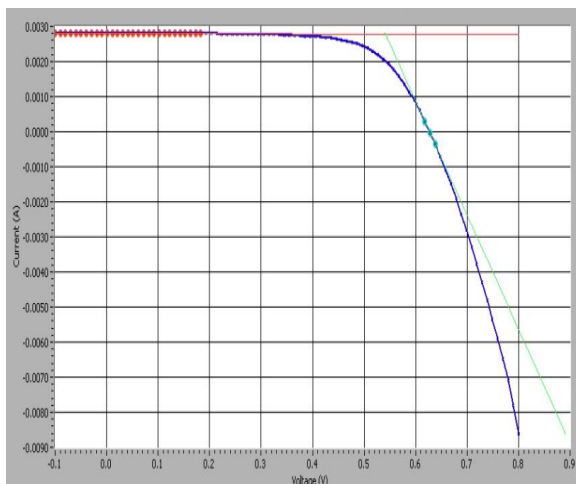
Voc (V)	0.6716
Isc (A)	0.0028
Jsc (mA/cm <sup>2</sup> )	10.9106
Imax (A)	0.0024
Vmax (V)	0.5195
Pmax (mW)	1.2572
Fill Factor (%)	65.9859
Efficiency (%)	4.8355
R at Voc	32.0477
R at Isc	5023.3692

DSSC which used N3 sensitizer (18 immersion hours)



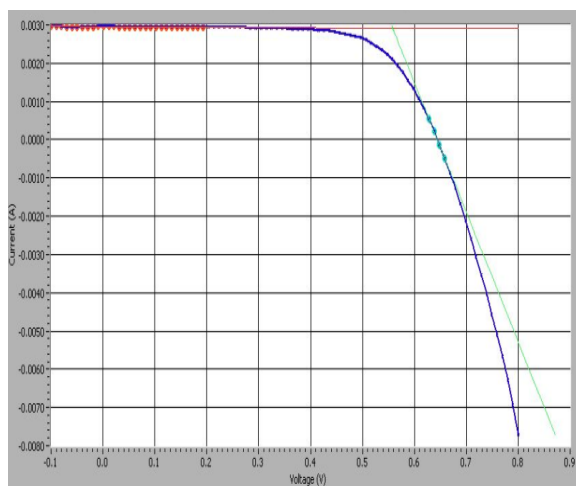
Voc (V)	0.6112
Isc (A)	0.0024
Jsc (mA/cm <sup>2</sup> )	14.2699
Imax (A)	0.0021
Vmax (V)	0.4743
Pmax (mW)	0.9734
Fill Factor (%)	65.6498
Efficiency (%)	5.7257
R at Voc	33.4809
R at Isc	5729.4009

DSSC which used N3 sensitizer (20 immersion hours)



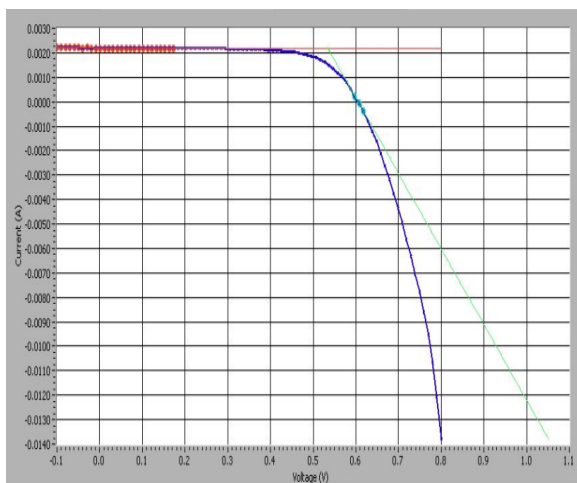
Voc (V)	0.6270
Isc (A)	0.0028
Jsc (mA/cm <sup>2</sup> )	14.0353
Imax (A)	0.0025
Vmax (V)	0.4864
Pmax (mW)	1.2178
Fill Factor (%)	69.2000
Efficiency (%)	6.0892
R at Voc	30.7380
R at Isc	21439.6438

DSSC which used N3 sensitizer (22 immersion hours)



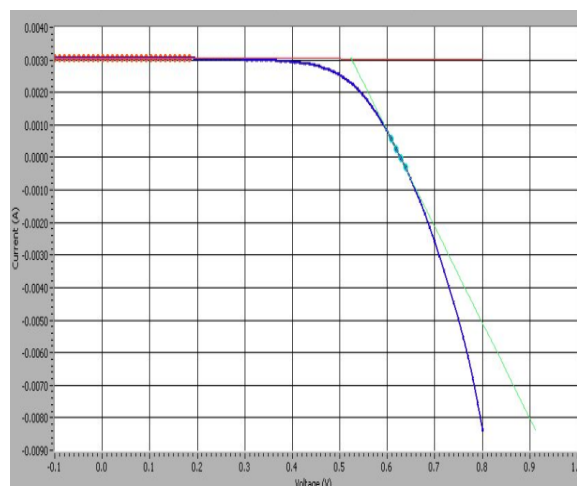
Voc (V)	0.6442
Isc (A)	0.0030
Jsc (mA/cm <sup>2</sup> )	14.7652
Imax (A)	0.0027
Vmax (V)	0.4986
Pmax (mW)	1.3224
Fill Factor (%)	69.5175
Efficiency (%)	6.6121
R at Voc	29.4837
R at Isc	15134.4095

DSSC which used N3 sensitizer (24 immersion hours)



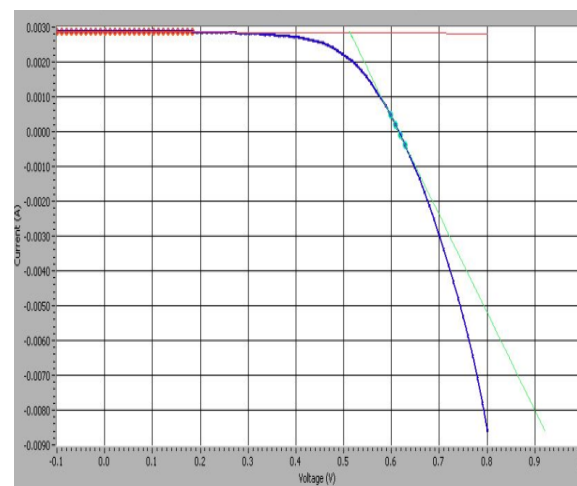
Voc (V)	0.6053
Isc (A)	0.0022
Jsc (mA/cm <sup>2</sup> )	14.6621
Imax (A)	0.0019
Vmax (V)	0.4806
Pmax (mW)	0.9341
Fill Factor (%)	70.1700
Efficiency (%)	6.2272
R at Voc	32.4002
R at Isc	19455.0198

DSSC which used N3 sensitizer (26 immersion hours)



Voc (V)	0.6275
Isc (A)	0.0031
Jsc (mA/cm <sup>2</sup> )	13.8818
Imax (A)	0.0027
Vmax (V)	0.4759
Pmax (mW)	1.2889
Fill Factor (%)	67.2588
Efficiency (%)	5.8586
R at Voc	33.9419
R at Isc	33099.4773

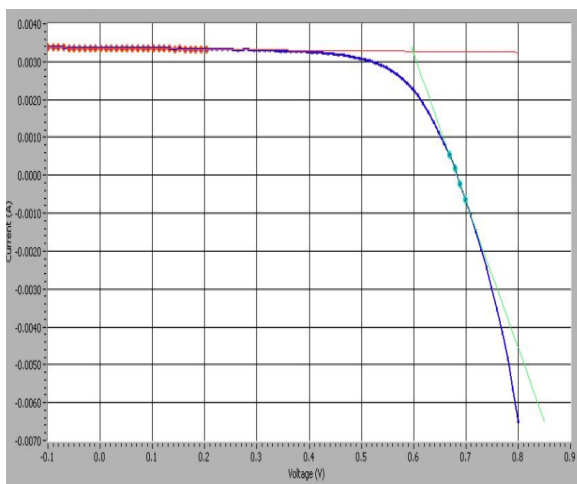
DSSC which used N3 sensitizer (28 immersion hours)



Voc (V)	0.6146
Isc (A)	0.0029
Jsc (mA/cm <sup>2</sup> )	14.0133
Imax (A)	0.0025
Vmax (V)	0.4606
Pmax (mW)	1.1556
Fill Factor (%)	65.4516
Efficiency (%)	5.6371
R at Voc	35.6911
R at Isc	14336.4055

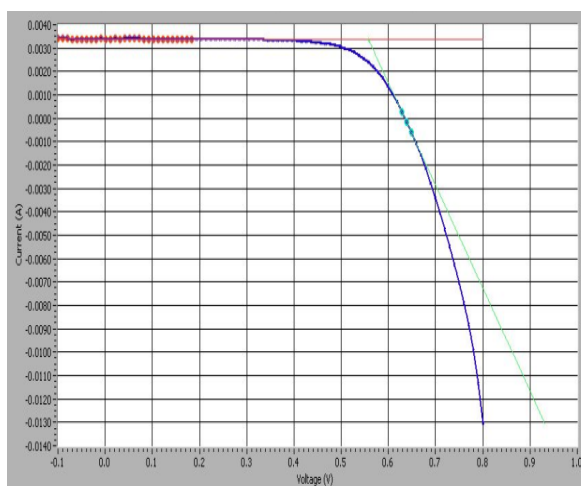
DSSC which used N3 sensitizer (30 immersion hours)

## APPENDIX H: I-V Test results for DSSC with N719



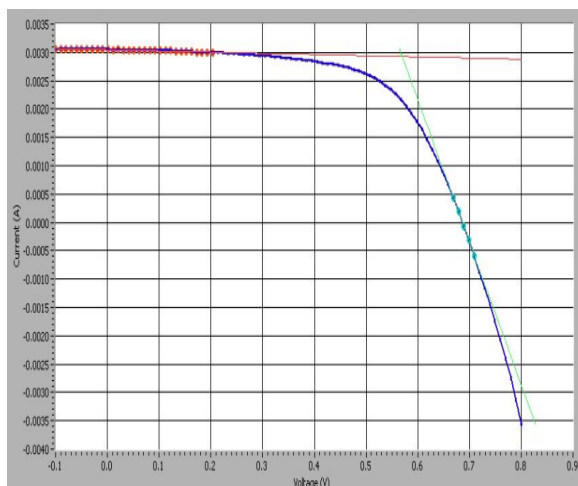
Voc (V)	0.6827
Isc (A)	0.0034
Jsc (mA/cm <sup>2</sup> )	11.9836
Imax (A)	0.0029
Vmax (V)	0.5322
Pmax (mW)	1.5650
Fill Factor (%)	68.3203
Efficiency (%)	5.5893
R at Voc	25.7458
R at Isc	7254.2957

DSSC which used N719 sensitizer (10 immersion hours)



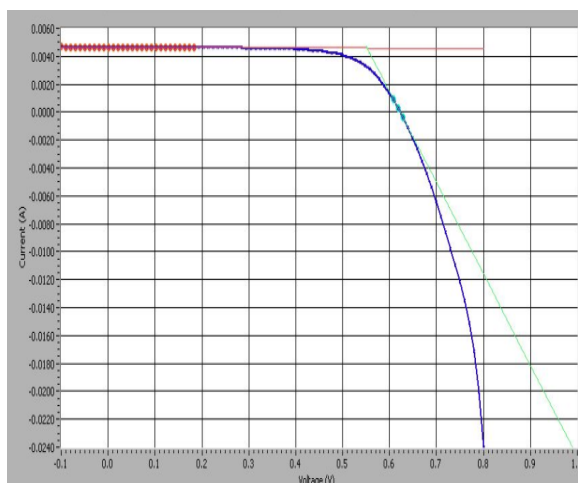
Voc (V)	0.6346
Isc (A)	0.0034
Jsc (mA/cm <sup>2</sup> )	12.5703
Imax (A)	0.0030
Vmax (V)	0.5000
Pmax (mW)	1.5244
Fill Factor (%)	70.7799
Efficiency (%)	5.6460
R at Voc	22.7912
R at Isc	53695.2630

DSSC which used N719 sensitizer (12 immersion hours)



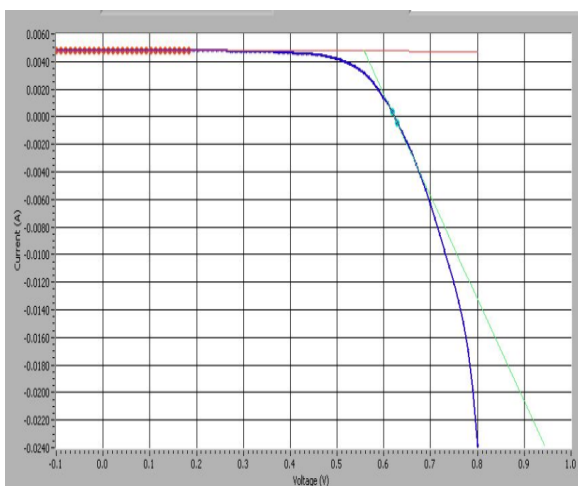
Voc (V)	0.6860
Isc (A)	0.0030
Jsc (mA/cm <sup>2</sup> )	13.8473
Imax (A)	0.0026
Vmax (V)	0.5138
Pmax (mW)	1.3134
Fill Factor (%)	62.8499
Efficiency (%)	5.9701
R at Voc	39.6069
R at Isc	4809.8720

DSSC which used N719 sensitizer (14 immersion hours)



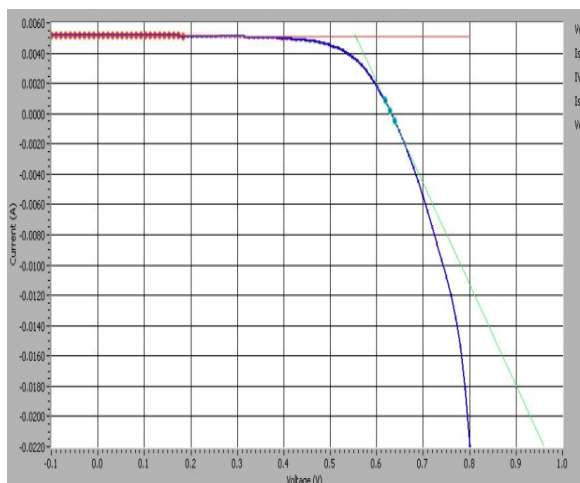
Voc (V)	0.6222
Isc (A)	0.0047
Jsc (mA/cm <sup>2</sup> )	16.6259
Imax (A)	0.0041
Vmax (V)	0.4938
Pmax (mW)	2.0440
Fill Factor (%)	70.5648
Efficiency (%)	7.3001
R at Voc	15.3496
R at Isc	8258.4391

DSSC which used N719 sensitizer (16 immersion hours)



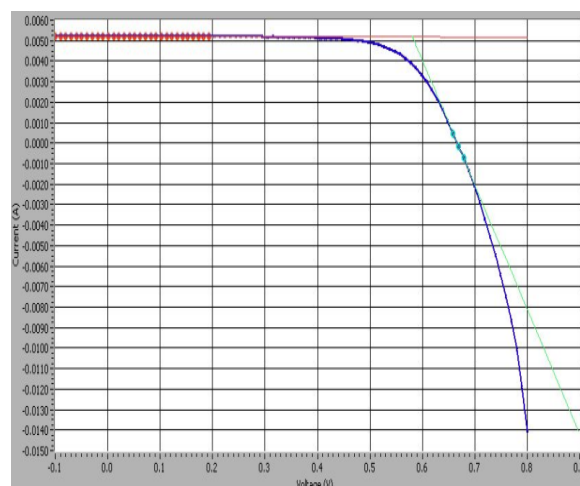
Voc (V)	0.6223
Isc (A)	0.0048
Jsc (mA/cm <sup>2</sup> )	17.1837
Imax (A)	0.0043
Vmax (V)	0.4936
Pmax (mW)	2.1039
Fill Factor (%)	70.2646
Efficiency (%)	7.5140
R at Voc	13.4607
R at Isc	10691.4392

DSSC which used N719 sensitizer (18 immersion hours)



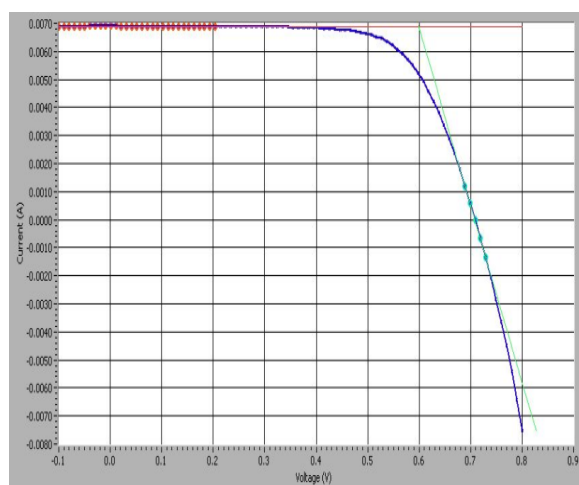
Voc (V)	0.6312
Isc (A)	0.0052
Jsc (mA/cm <sup>2</sup> )	17.1720
Imax (A)	0.0046
Vmax (V)	0.4957
Pmax (mW)	2.2638
Fill Factor (%)	69.6210
Efficiency (%)	7.5460
R at Voc	14.9707
R at Isc	15010.2524

DSSC which used N719 sensitizer (20 immersion hours)



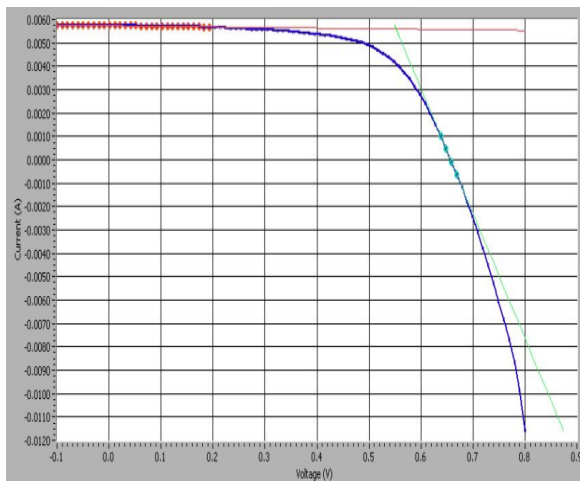
Voc (V)	0.6665
Isc (A)	0.0052
Jsc (mA/cm <sup>2</sup> )	17.3883
Imax (A)	0.0047
Vmax (V)	0.5267
Pmax (mW)	2.4869
Fill Factor (%)	71.5263
Efficiency (%)	8.2898
R at Voc	16.4294
R at Isc	18186.2670

DSSC which used N719 sensitizer (22 immersion hours)



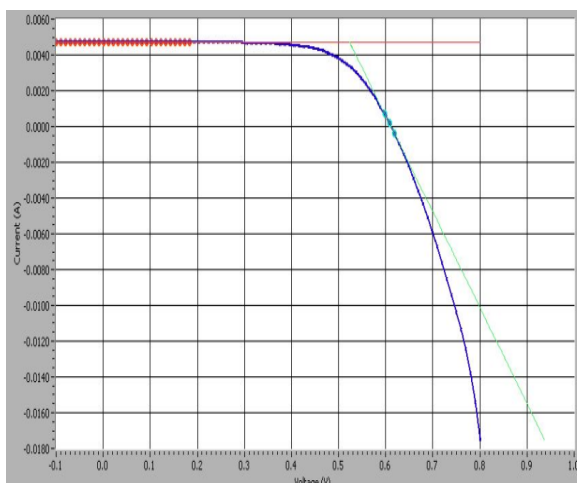
Voc (V)	0.7082
Isc (A)	0.0069
Jsc (mA/cm <sup>2</sup> )	17.2311
Imax (A)	0.0063
Vmax (V)	0.5411
Pmax (mW)	3.4115
Fill Factor (%)	69.8920
Efficiency (%)	8.5288
R at Voc	15.8354
R at Isc	25620.6835

DSSC which used N719 sensitizer (24 immersion hours)



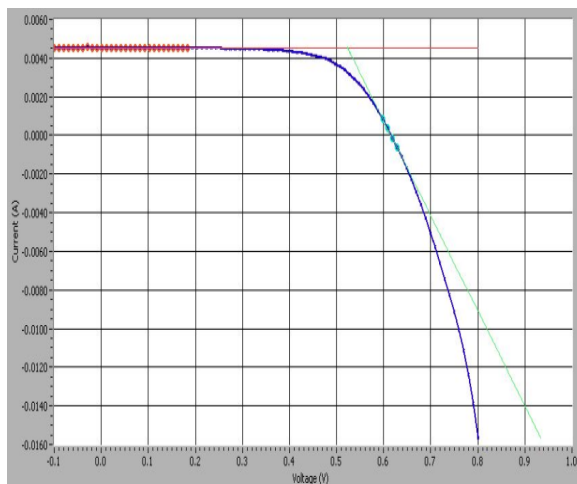
Voc (V)	0.6571
Isc (A)	0.0057
Jsc (mA/cm <sup>2</sup> )	18.5156
Imax (A)	0.0049
Vmax (V)	0.5009
Pmax (mW)	2.4452
Fill Factor (%)	64.8342
Efficiency (%)	7.8878
R at Voc	18.7362
R at Isc	3914.5001

DSSC which used N719 sensitizer (26 immersion hours)



Voc (V)	0.6110
Isc (A)	0.0047
Jsc (mA/cm <sup>2</sup> )	18.1939
Imax (A)	0.0042
Vmax (V)	0.4674
Pmax (mW)	1.9758
Fill Factor (%)	68.3536
Efficiency (%)	7.5991
R at Voc	18.6508
R at Isc	19212.1420

DSSC which used N719 sensitizer (28 immersion hours)



Voc (V)	0.6155
Isc (A)	0.0045
Jsc (mA/cm <sup>2</sup> )	17.4690
Imax (A)	0.0040
Vmax (V)	0.4687
Pmax (mW)	1.8898
Fill Factor (%)	67.6011
Efficiency (%)	7.2686
R at Voc	20.3061
R at Isc	19672.0028

DSSC which used N719 sensitizer (30 immersion hours)